The X_{17} search with the PADME experiment

Marco Mancini – LNF-INFN on behalf of the Collaboration

July 11, 2024 – IDM2024, L'Aquila-Italy

marco.mancini@lnf.infn.it

The Dark Matter problem and portals physics

Dark Matter indirect evidences → **two main solutions**

1. **Weakly Interacting Massive Particles** (WIMPs)
2. **Light Dark Matter** (LDM)
   - MeV-GeV "hidden-sector" states
   - Neutral under SM interactions but
   - Interacting with SM via **new forces**
   - Classified on an effective-interaction basis

Portal	Coupling
Dark photon, A_μ	$-\frac{\epsilon}{2\cos\theta_W}F'_{\mu\nu}B^{\mu\nu}$
Dark Higgs, S	$(\mu S + \lambda S^2)H^\dagger H$
Axion, a	$\frac{a}{f_a}F_{\mu\nu}\tilde{F}^{\mu\nu}$, $\frac{a}{f_a}G_{i,\mu\nu}\tilde{G}_i^{\mu\nu}$, $\frac{\partial_\mu a}{f_a}\bar{\psi}\gamma^\mu\gamma^5\psi$
Sterile neutrino, N	$y_N LHN$

Phenomenology can hugely vary due to

- structure of the hidden sector
- simultaneous presence of many mediators
- mass structure, e.g. 2 M_{DM} < or > $M_{A'}$

Broadly speaking:

- Visible decays to SM particles
- Invisible decays (+ visible but long-lived)

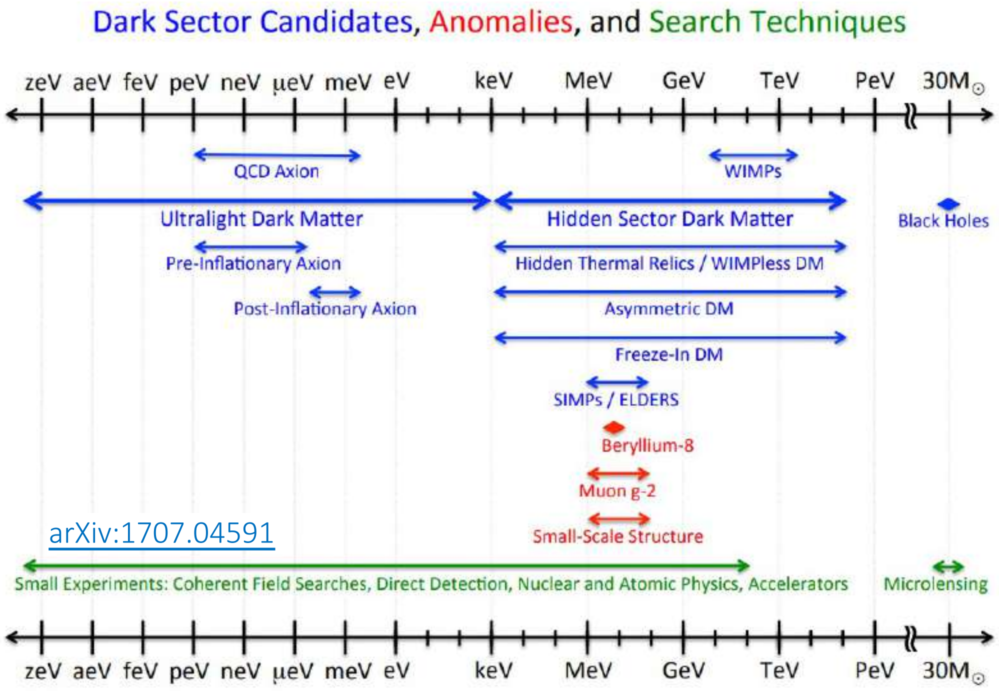

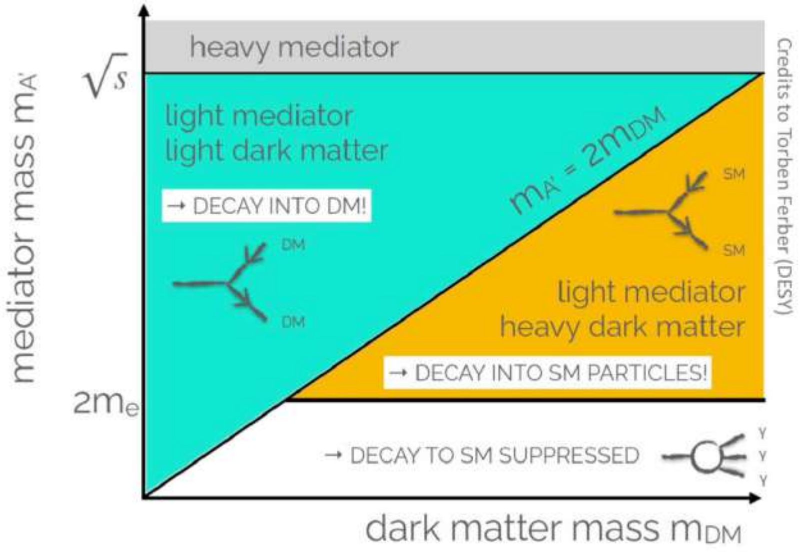

The ATOMKI X_{17} anomaly

Anomaly in the angular correlation of e^+e^- pairs emitted via IPC in the ^8Be, ^4He and ^{12}C nuclear de-excitation. It seems to be compatible with a **new** $\sim$ **17 MeV** mass neutral mediator

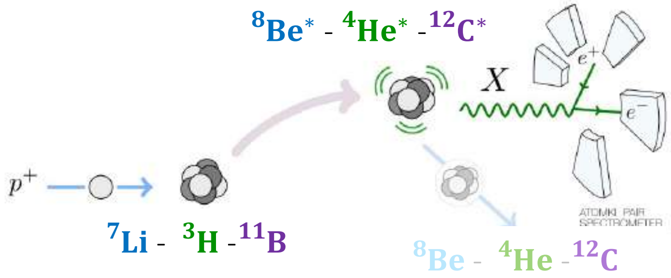

Phys.Rev.Lett. 116 (2016) 4, 042501

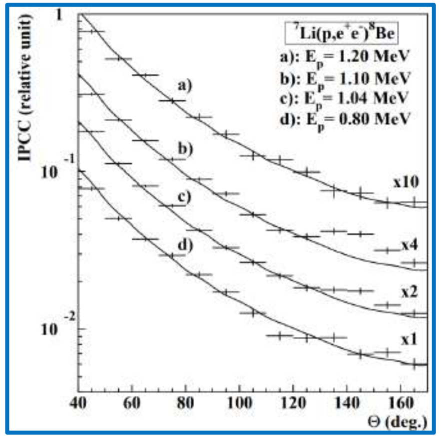

Phys.Rev.C, 104(4):044003

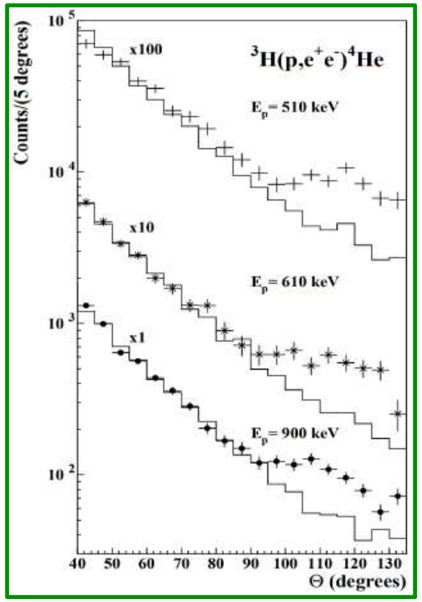

Phys. Rev. C 106, L061601

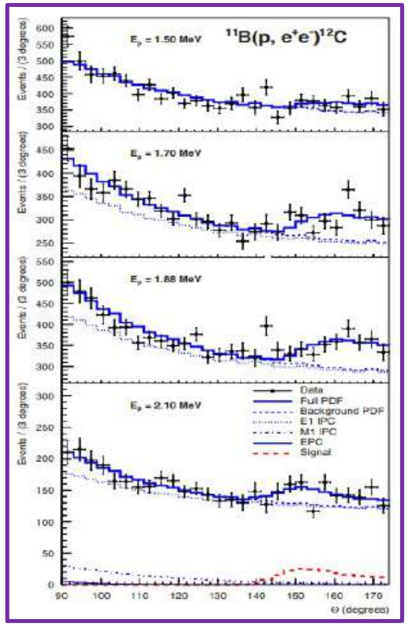

PHYSICAL REVIEW D **102**, 036016 (2020)

Dynamical evidence for a fifth force explanation of the ATOMKI nuclear anomalies

Jonathan L. Feng,* Tim M. P. Tait,† and Christopher B. Verhaaren‡
Department of Physics and Astronomy, University of California, Irvine, California 92697-4575, USA

Feng et al. suggested that X_{17} should be observed in ^{12}C transitions
X_{17} observations in ^{12}C will point to a vector or axial vector nature for X_{17}

Feng et al., Phys.Rev.D 102 (2020) 3, 036016

TABLE III. Nuclear excited states N_*, their spin-parity $J_*^{P_*}$, and the possibilities for X (scalar, pseudoscalar, vector, axial vector) allowed by angular momentum and parity conservation, along with the operators that mediate the decay and references to the equation numbers where these operators are defined. The operator subscripts label the operator's dimension and the partial wave of the decay, and the superscript labels the X spin. For example, $\mathcal{O}_{4P}^{(0)}$ is a dimension-four operator that mediates a P-wave decay to a spin-0 X boson.

N_*	$J_*^{P_*}$	Scalar X	Pseudoscalar X	Vector X	Axial Vector X
^{8}Be(18.15)	1^+	…	$\mathcal{O}_{4P}^{(0)}$ (27)	$\mathcal{O}_{5P}^{(1)}$ (37)	$\mathcal{O}_{3S}^{(1)}$ (29), $\mathcal{O}_{5D}^{(1)}$ (34)
^{12}C(17.23)	1^-	$\mathcal{O}_{4P}^{(0)}$ (27)	…	$\mathcal{O}_{3S}^{(1)}$ (29), $\mathcal{O}_{5D}^{(1)}$ (34)	$\mathcal{O}_{5P}^{(1)}$ (37)
^{4}He(21.01)	0^-	…	$\mathcal{O}_{3S}^{(0)}$ (39)	…	$\mathcal{O}_{4P}^{(1)}$ (40)
^{4}He(20.21)	0^+	$\mathcal{O}_{3S}^{(0)}$ (39)	…	$\mathcal{O}_{4P}^{(1)}$ (40)	…

Searching for X_{17} using resonant production

Two different production mechanisms, annihilation and emission:

- Resonant annihilation: $e^+e^- \rightarrow A' \rightarrow \sigma_{res}(E_{e^+}) = \frac{12\pi}{m_{A'}^2} \frac{\Gamma_{A'}^2/4}{\left(\sqrt{s}-m_{A'}\right)^2+\Gamma_{A'}^2/4}$

  Nardi et al. Phys. Rev. D 97, 095004
- Associated production: $e^+e^- \rightarrow \gamma A'$
- A'-strahlung: $e^\pm Z \rightarrow e^\pm Z A'$

The resonant annihilation is accessible only with a positron-beam facility

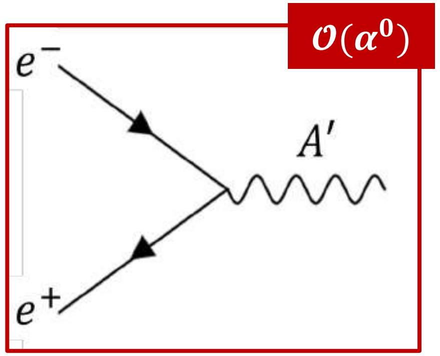

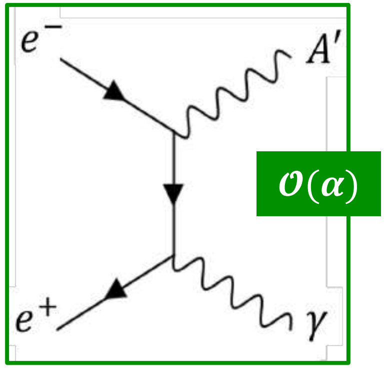

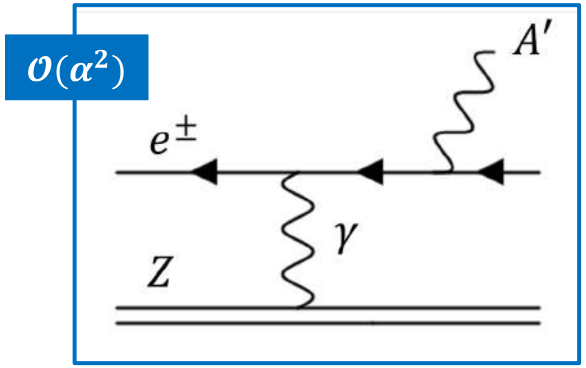

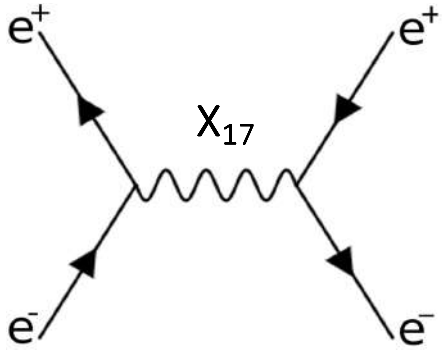

PADME Run III analysis strategy: vary the beam energy, fit the bkg, calibrate the luminosity and look for a bump from visible X_{17} decay in e^+e^-. The $\sqrt{s}$ should be as close as possible to the expected mass : $E_{res} \sim \frac{m_{X17}^2}{2m_e}$ → A scanning procedure is required

Searching for X_{17} using resonant production

Resonant cross section in (target) electron at rest approximation → large number of X_{17} **event**

[Darme et al. Phys. Rev. D 106, 115036](#)

$$N^{perPoT}_{vector} \simeq \frac{g_{Ve}^2}{2m_e}\,\ell_{tar}\,\frac{N_A \rho Z}{A}\,f(E_{res},E_{beam}) \sim 1.8\times10^{-7}\times\left(\frac{g_{ve}}{2\cdot10^{-4}}\right)^2\left(\frac{1\ \mathrm{MeV}}{\sigma_E}\right)$$

$$N^{perPoT}_{ALP} \simeq 5.8\times10^{-7}\times\left(\frac{g_{ae}}{\mathrm{GeV}^{-1}}\right)^2\left(\frac{1\ \mathrm{MeV}}{\sigma_E}\right)$$

$f(E_{res},E_{beam})$ is a gaussian describing the beam energy distribution with spread σ_E

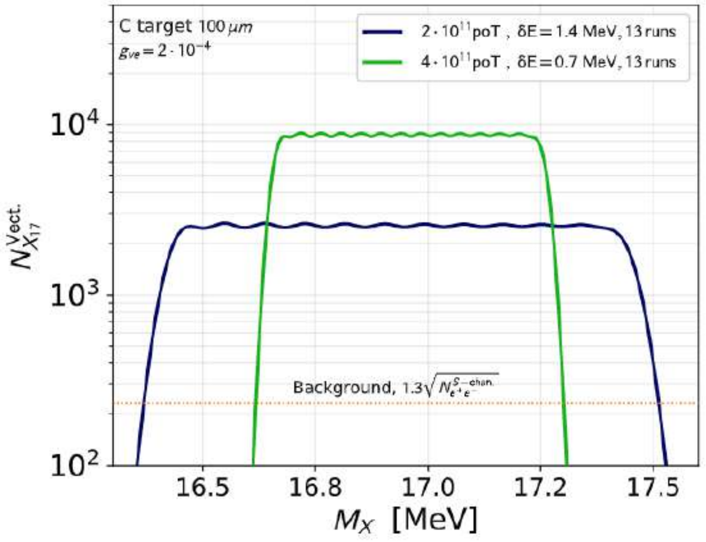

Fixed target experiment: ***s*- and *t*- channel kinematics can be distinguished**

- X_{17} resonant production has same acceptance of Bhabha *s*-channel
- Full Bhabha scattering strongly boosted in forward direction
- Set of cuts selecting events where bkg yield is comparable to the signal

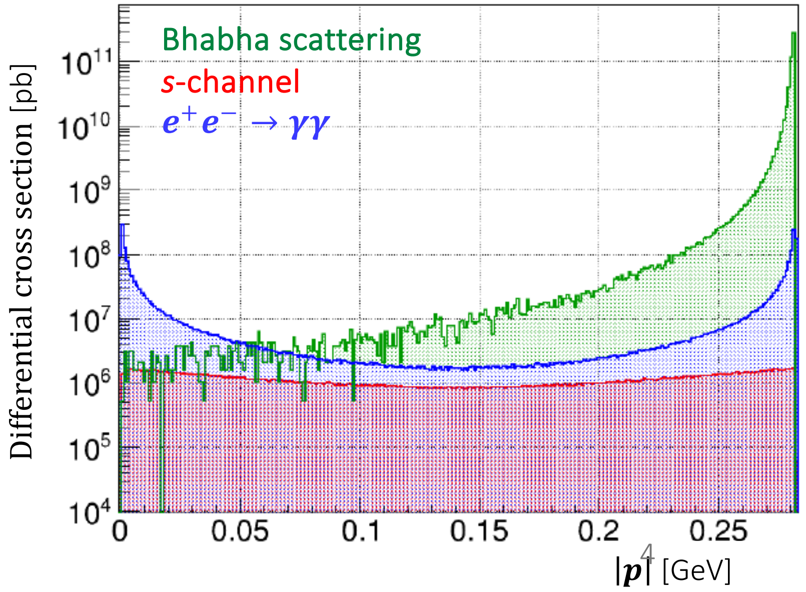

Dedicated experimental setup

The Run III experimental set-up

More on PADME: 2022 JINST 17 P08032, arXiv:2405.07203

Setup to search for the X_{17} in the resonant annihilation $e^+e^- \rightarrow X_{17} \rightarrow e^+e^-$

- e^+-beam ($\mathbf{200 < \mathit{E} < 405}$ MeV) on $\mathbf{100\ \mu m}$ active diamond target
- Low beam multiplicity $\sim 3\times10^3$ PoT per bunch
- Dipole $\boldsymbol{B}$-field off
- Signal → 2 EM clusters in ECal
- TimePix3 beam monitor and PbGl luminometer at the end of the beam line
- ETagger detector in front of ECal to distinguish $e^{\pm}$ from γ

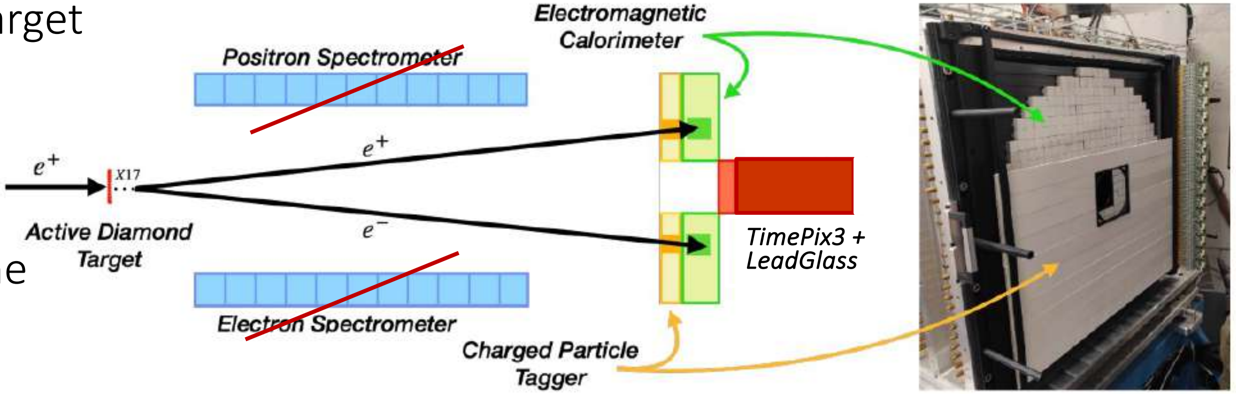

OBSERVABLES

$$\left\{\begin{array}{l} \dfrac{N(e^+e^-)}{N^{PoT}} \ \mathbf{vs}\ \sqrt{s} \\[2ex] \boxed{\dfrac{N(e^+e^-+\gamma\gamma)}{N^{PoT}} \ \mathbf{vs}\ \sqrt{s}} \\[2ex] \dfrac{N(e^+e^-)}{N(\gamma\gamma)} \ \mathbf{vs}\ \sqrt{s} \end{array}\right.$$

RUN 3

e^+ beam

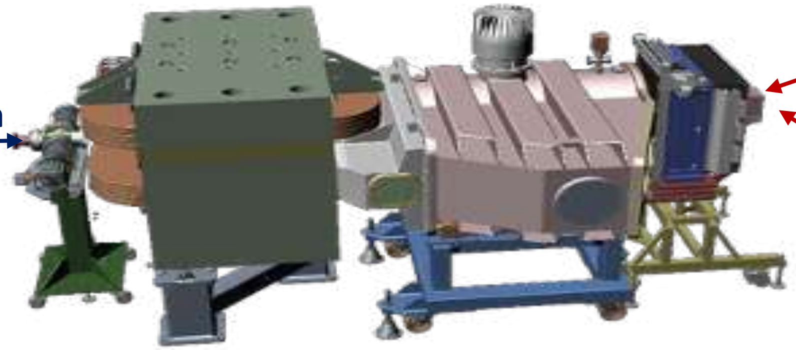

PbGl luminometer

TimePix3

Components in the analysis:

- **Signal selection** and **events identification** → **Bkg contribution**
- Determination of the **normalization** → **PADME luminosity measurement**
- **Expected signal yield** → Theoretical input: X_{17} line shape

Run III collected data – winter 2022

Total amount of collected data is $\sim 6{\times}10^{11}$ PoT, i.e. $\sim 10^{10}$ PoT per $\sqrt{s}$ point:

- 47 points in $260\ \text{MeV} < E_{Beam} < 300\ \text{MeV}$ and $\delta E_{Beam} \sim 0.75\ \text{MeV}$ energy step → on-resonance region
- **6 points out-of-resonance**, where the X_{17} production is forbidden:
  - 5 points with $\sim 10^{10}$ PoT each and $205\ \text{MeV} \leq E_{Beam} \leq 212\ \text{MeV}$
  - 1 point with $\sim 2{\times}10^{10}$ PoT and $E_{Beam} = 402\ \text{MeV}$

PADME can use out-of-resonance dataset to:

- Compare data and MC predictions
- Study the SM bkg
- Measure SM cross-section with no eventual X_{17} enhancement
- Tune the search technique
- Establish luminosity measurement precision

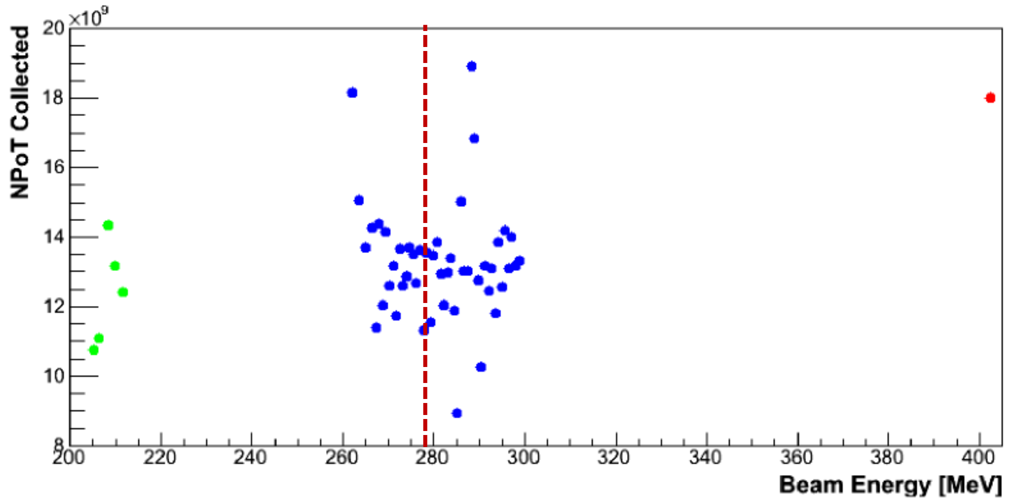

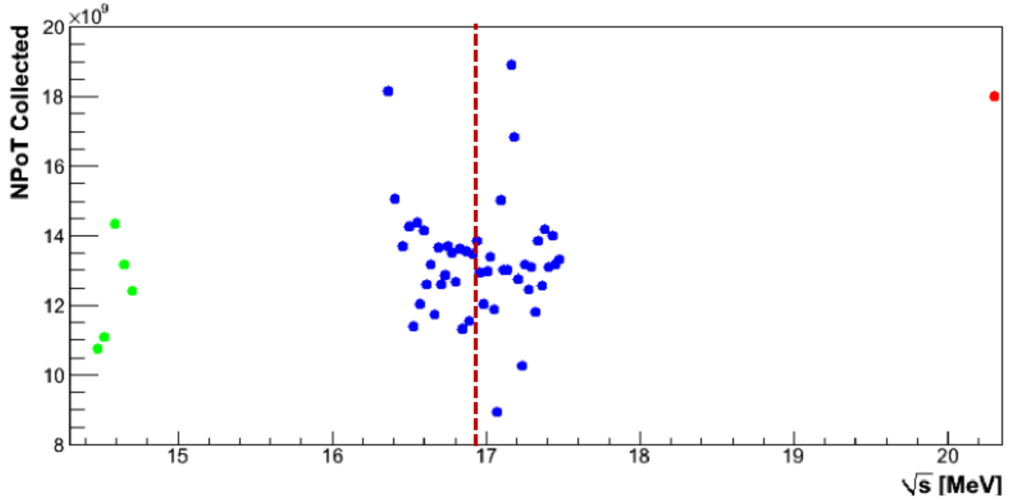

$m_{X_{17}} = 16.85 \pm 0.04$ MeV

Phys. Rev. D 108, 015009

Signal selection $N(2CL) = N(e^+e^- + \gamma\gamma)$

ECal based selection aimed at N(2CL)/N^{PoT} studies:

- Info on detector operation stability and acceptance during the data taking
- 2 in time clusters in the $\boldsymbol{\Delta t} < \mathbf{5\ ns}$ in ECal
- **Energy** and **radius cuts**, **Center of Gravity (CoG)** consistency
- Cluster energy vs angle correlation compatible with a **2 body final state**

Background estimation (Bremmstrahlung + BIB) $\sim 4\ \%$

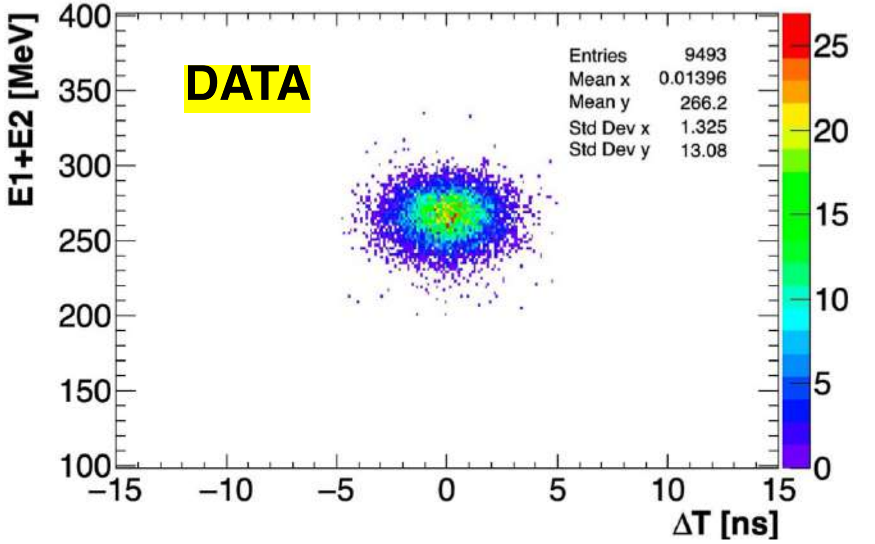

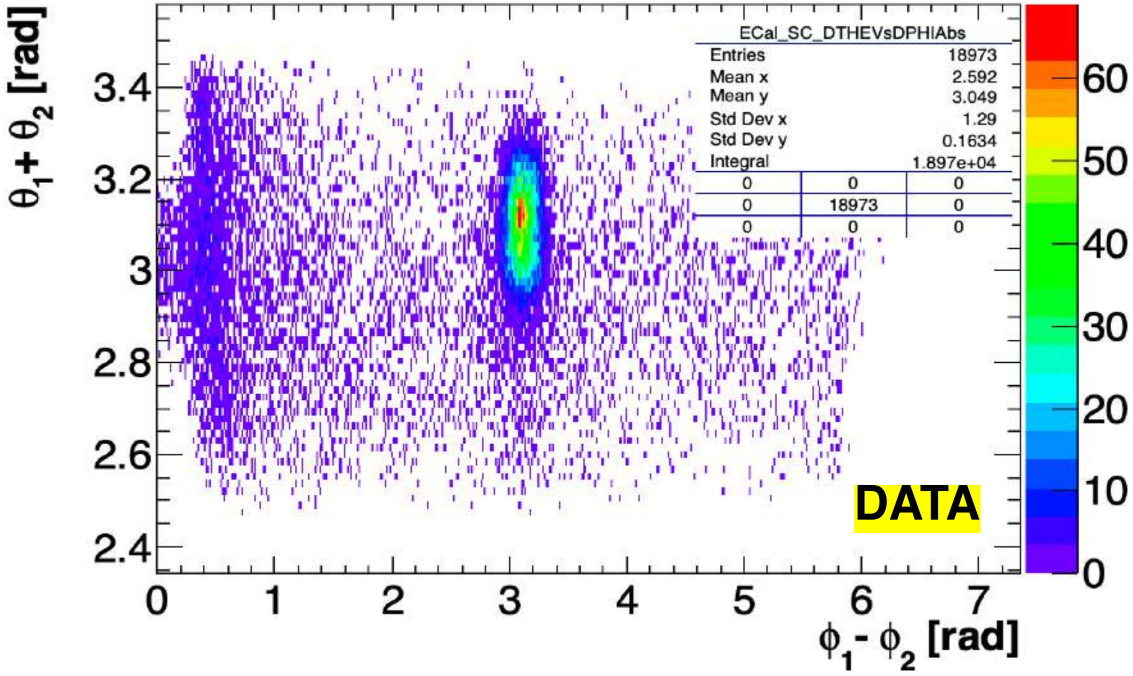

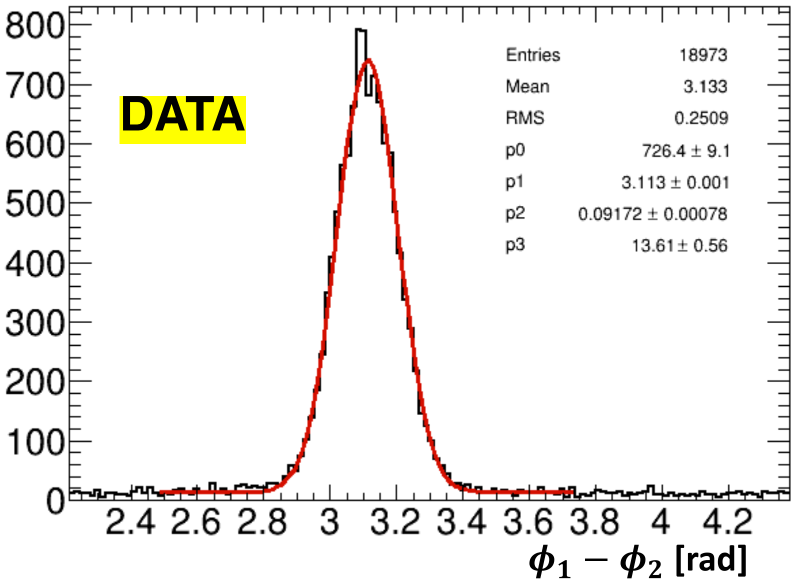

Signal selection: efficiency

Cluster reconstruction efficiency:
TAG&PROBE with DATA

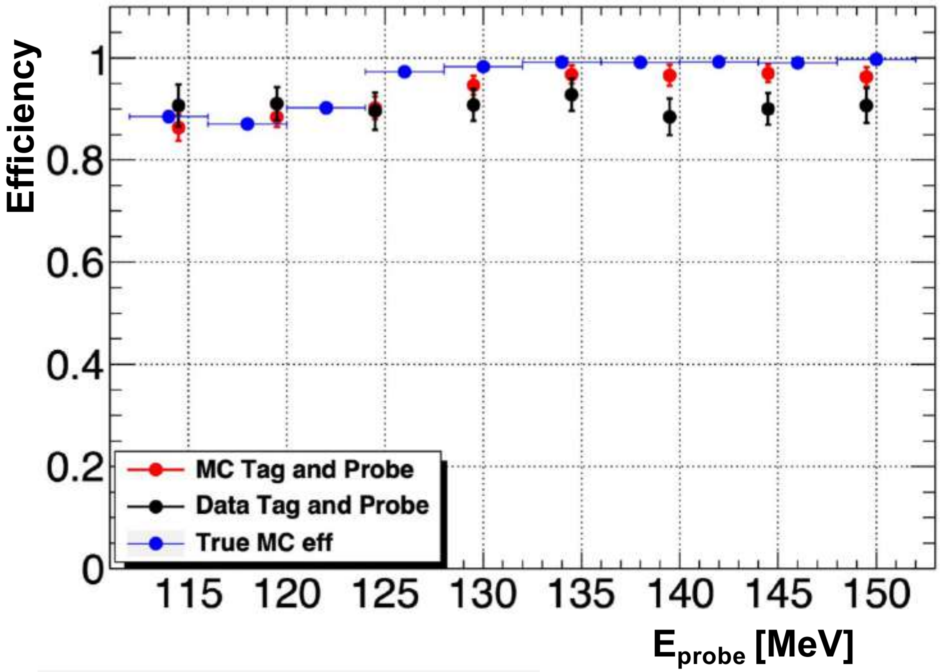

- Single hit identification threshold of $15\ \mathrm{MeV}$
- Cluster reconstruction efficiency is stable over time
- Bad crystals excluded from the reconstruction

Geometrical efficiency (**acceptance**)

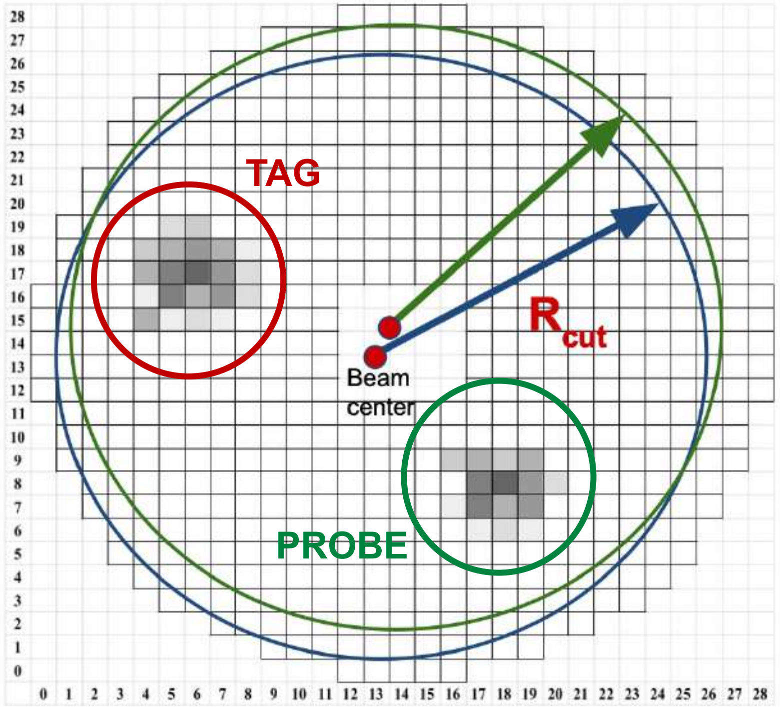

- Signal selection region in a corona centred on Centre of Gravity (**CoG**)
- Dominated by the cut on the outer radius of a cluster in the calorimeter
- Beam center drift limits the maximal R_{cut}

Signal and background: MC study

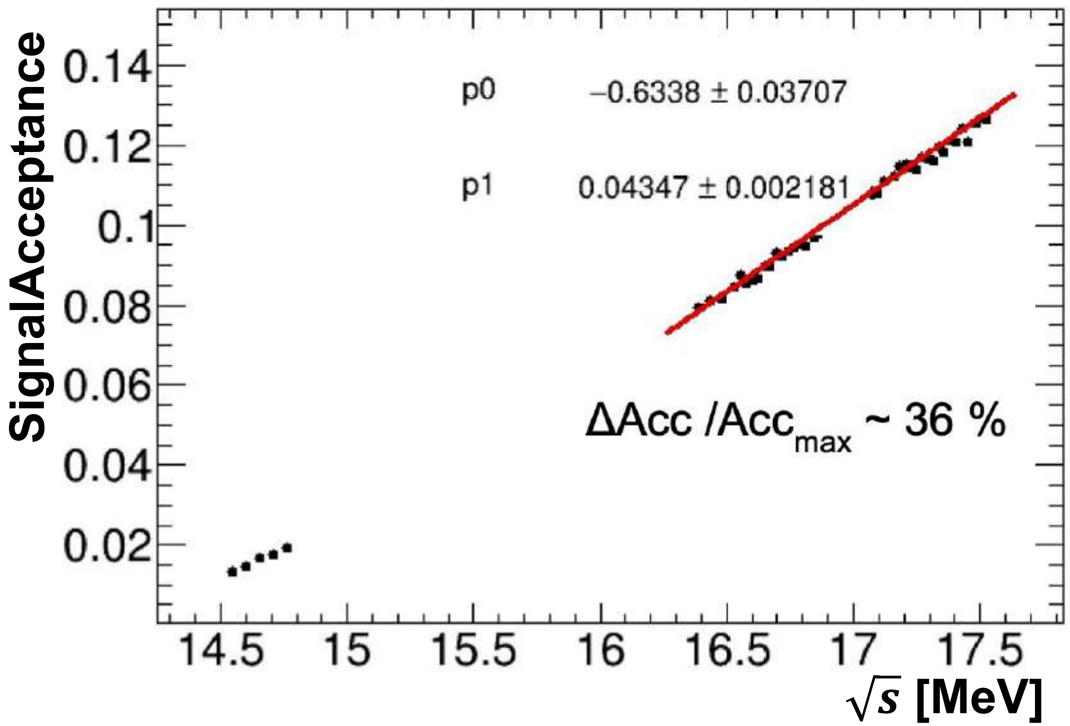

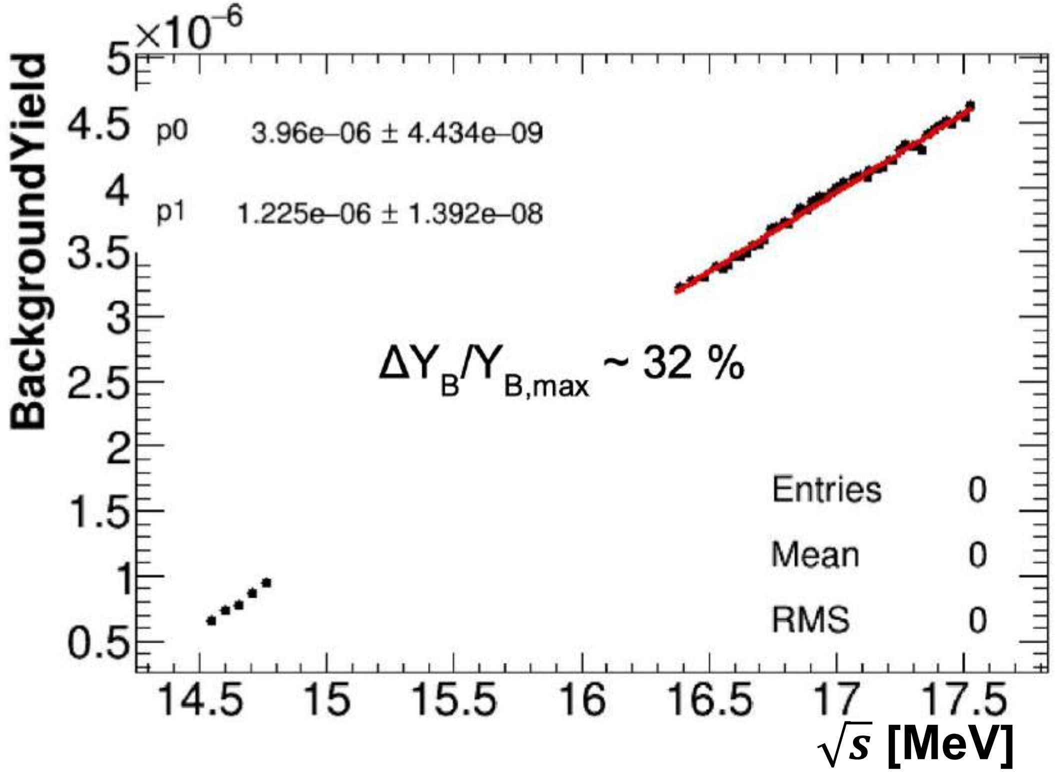

- Signal acceptance of the level of $\mathcal{O}(10\%)$
- Background contribution of the order of ∼40000 events per invariant mass point
- Both are dependent on the e^+e^- invariant mass
  - Accidental cancellation in the Signal/Bkg ratio, for a fixed g_{Ve}
- The **total uncertainty is of** $\mathcal{O}(1\%)$

Beam position monitoring

TimePix 3 array

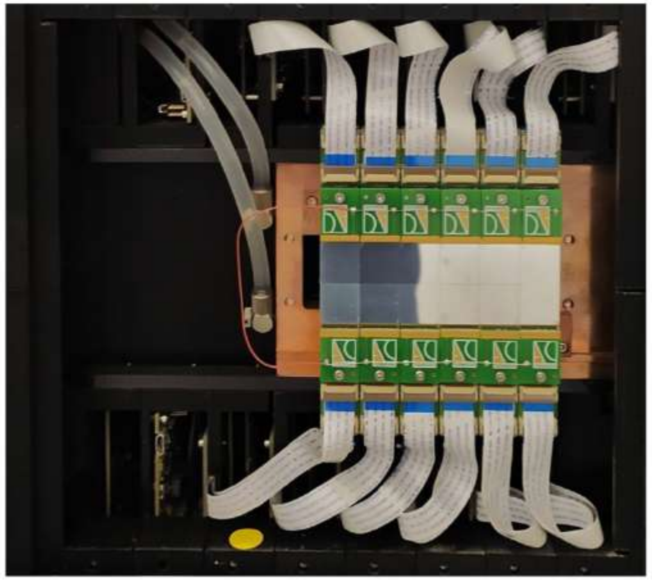

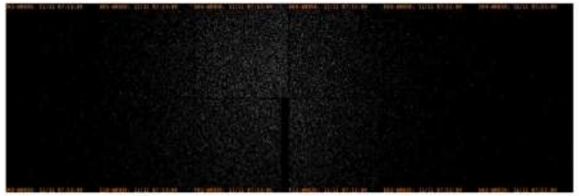

Matrix of 2x6 TimePix3 detectors (each 256x256 pixels)
Operated in 2 modes:

- Image mode → integrating
- Streaming mode → feeding ToT and ToA for each fired pixel

JINST 19 (2024) 01, C01016

CoG at the ECal front face from **2 cluster events**

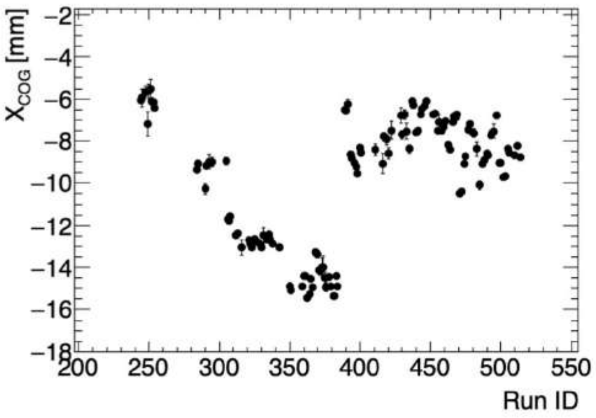

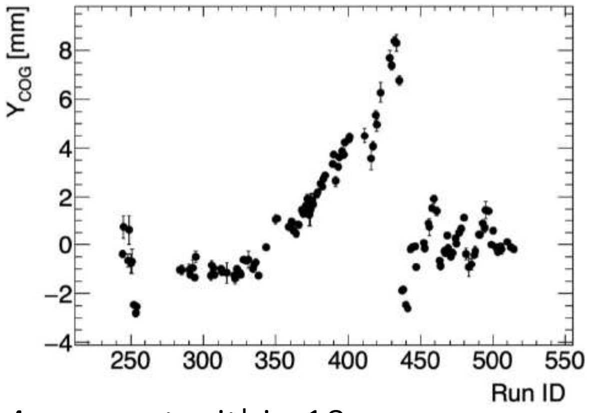

Movement within 10 mm

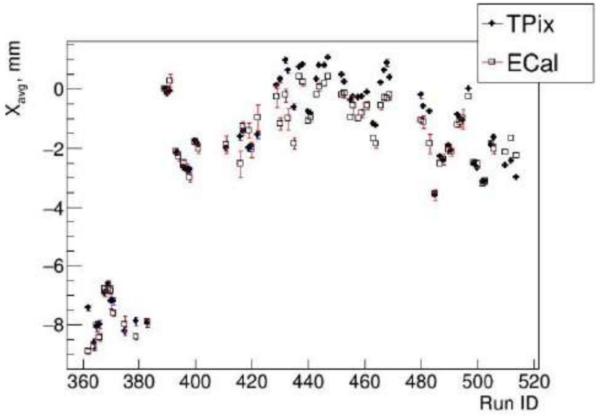

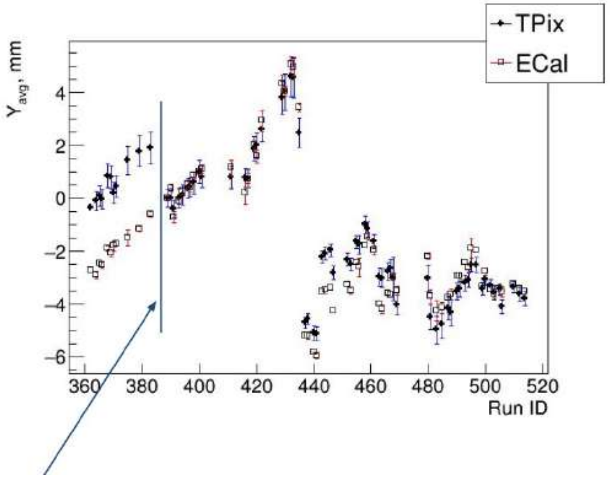

TimePix was moved by 1.8 mm → **Recovered**

arXiv:2405.07203

Positron flux measurement

Calibration of the PbGl @650 V with respect to the FitPix (BTF beam monitor) and data corrected accounting for the high positron density

- Validated with ToyMC and an independent measurement from BTF luminometer

Correction uncertainty of the order of $\sim 1\%$

- Common to all the measurements
- $Q_{1e} = (0.235 \pm 0.0043)$ pC

Uncertainty on $Q_{1e} < 2\%$

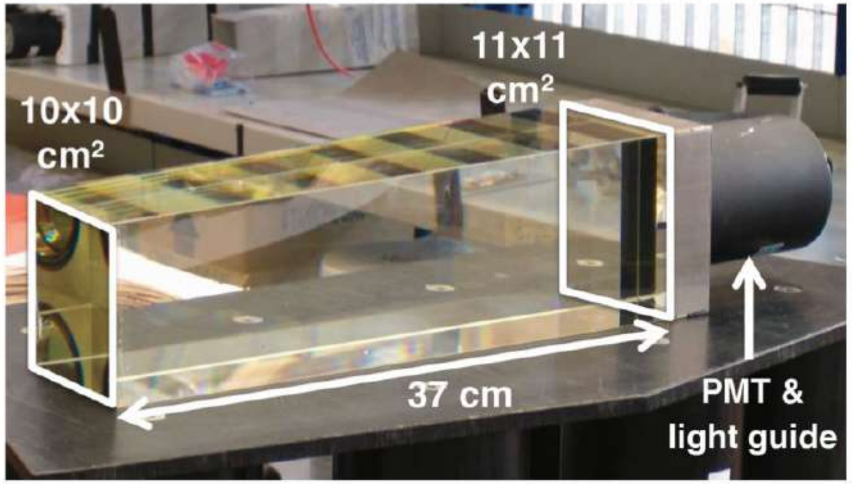

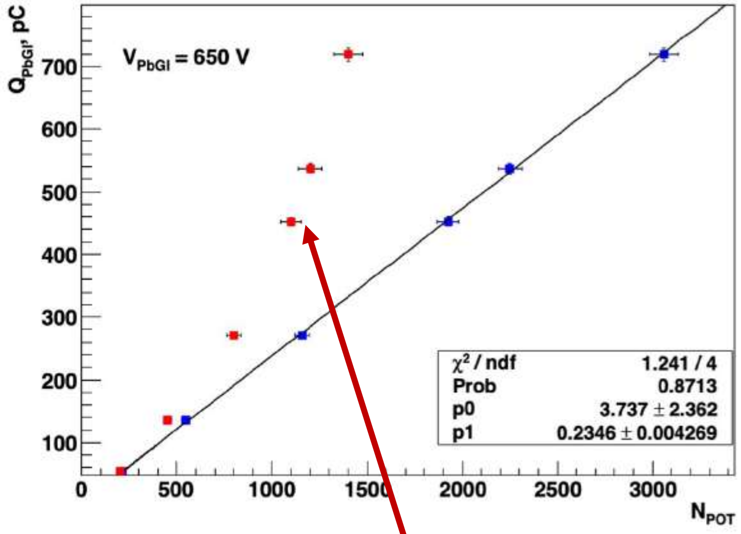

Before occupation correction

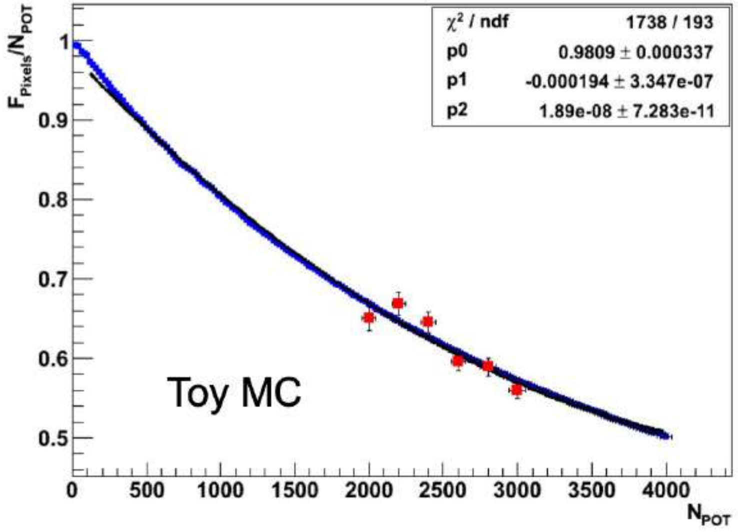

arXiv:2405.07203

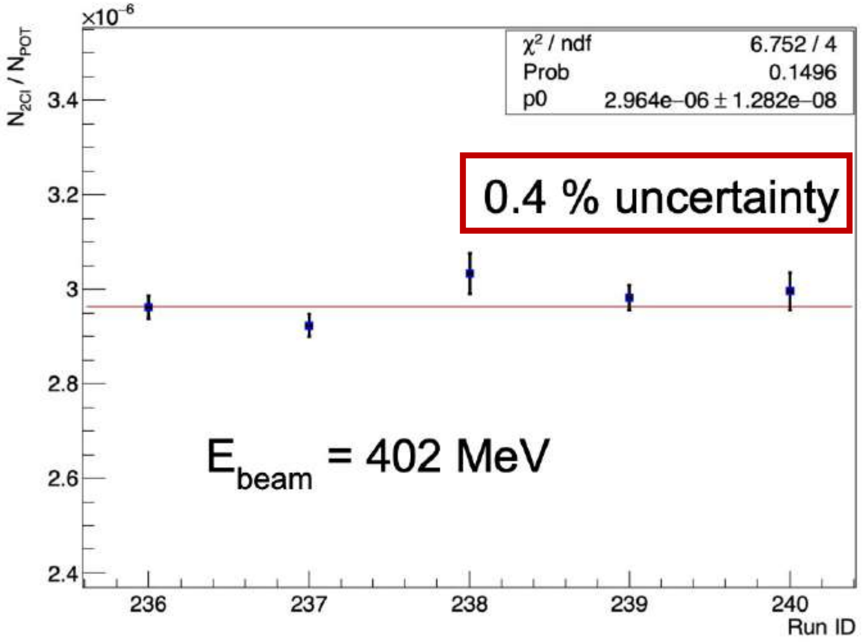

An unexpected phenomenon: electron motion

TOR VERGATA UNIVERSITÀ DEGLI STUDI DI ROMA · INFN LNF · PADME

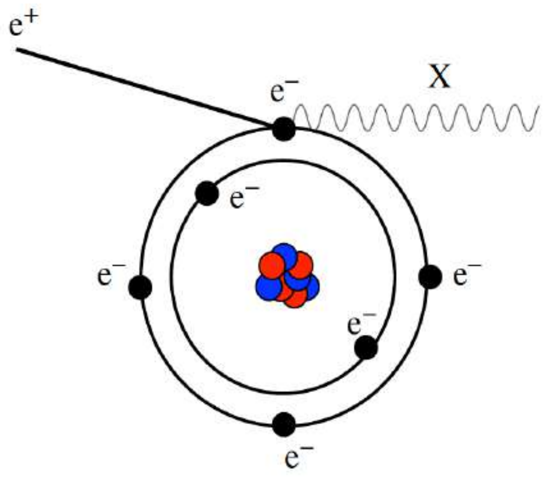

$$d\sigma = \frac{d^3 p_X}{(2\pi)^3} \int \frac{d^3 k_A}{(2\pi)^3} \frac{(2\pi)^4}{8 E_X E_A E_B |v_A - v_B|} \boxed{n(\vec{k}_A)} |\mathcal{M}|^2 \delta^4(k_A + p_B - p_X)$$

$\boxed{n(\vec{k}_A)}$

→ **Theory**: use Slater Type Orbitals, hybridization, Hartree Fock computations for atomic carbon, …

→ **Data**: obtain $n(\vec{k}_A)$ from data: Compton Profile, electron momentum distributions

X-Ray determination of the Electron Momentum Density in Diamond, Graphite and Carbon Black [Phys. Rev. 176 (1968) 900]

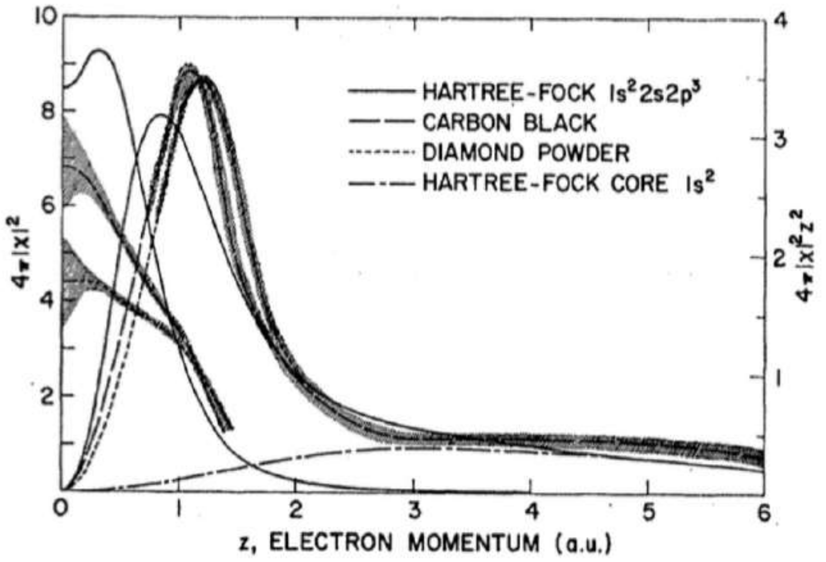

Theoretical Compton profile of diamond, boron nitride and carbon nitride [Physica B 521 (2017) 361-364]

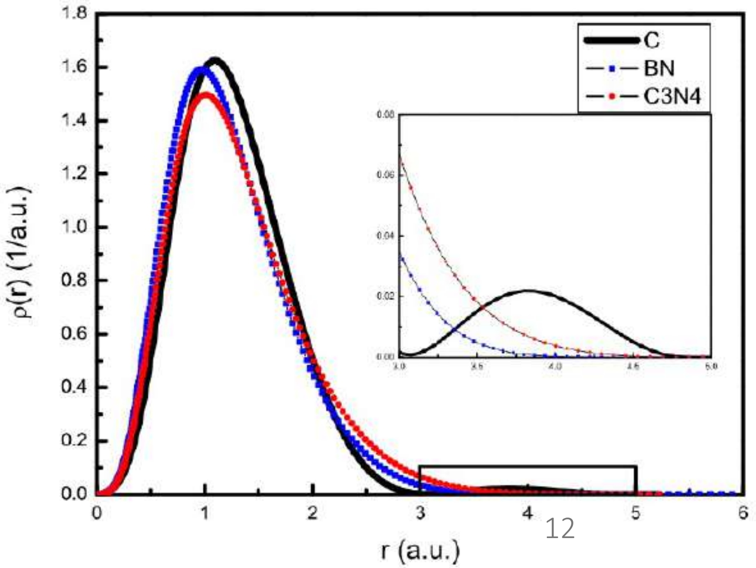

Line shape modification

- Bound e^- momentum changes the e^+e^- invariant mass → Signal/Bkg worsenes

$n(\vec{k}_A)$:

- **Theory**: calculate it using Hartree-Fock
- **Data**: X-ray determination of electron momentum density

[L. Darmé, G. Grilli di Cortona et al arXiv:2403.15387]

Sensitivity estimation

Sensitivity depends on Signal/Bkg and the uncertainty on the background determination:

- Statistical (N_{bkg}), 47 points with $\mathcal{O}(10^{10})$ PoT, $\Delta E_{beam} \simeq 0.75$ MeV
- Systematics (e.g. N^{PoT})
- Background: $N_{bkg} \sim 45000$ events per point
- Signal acceptance

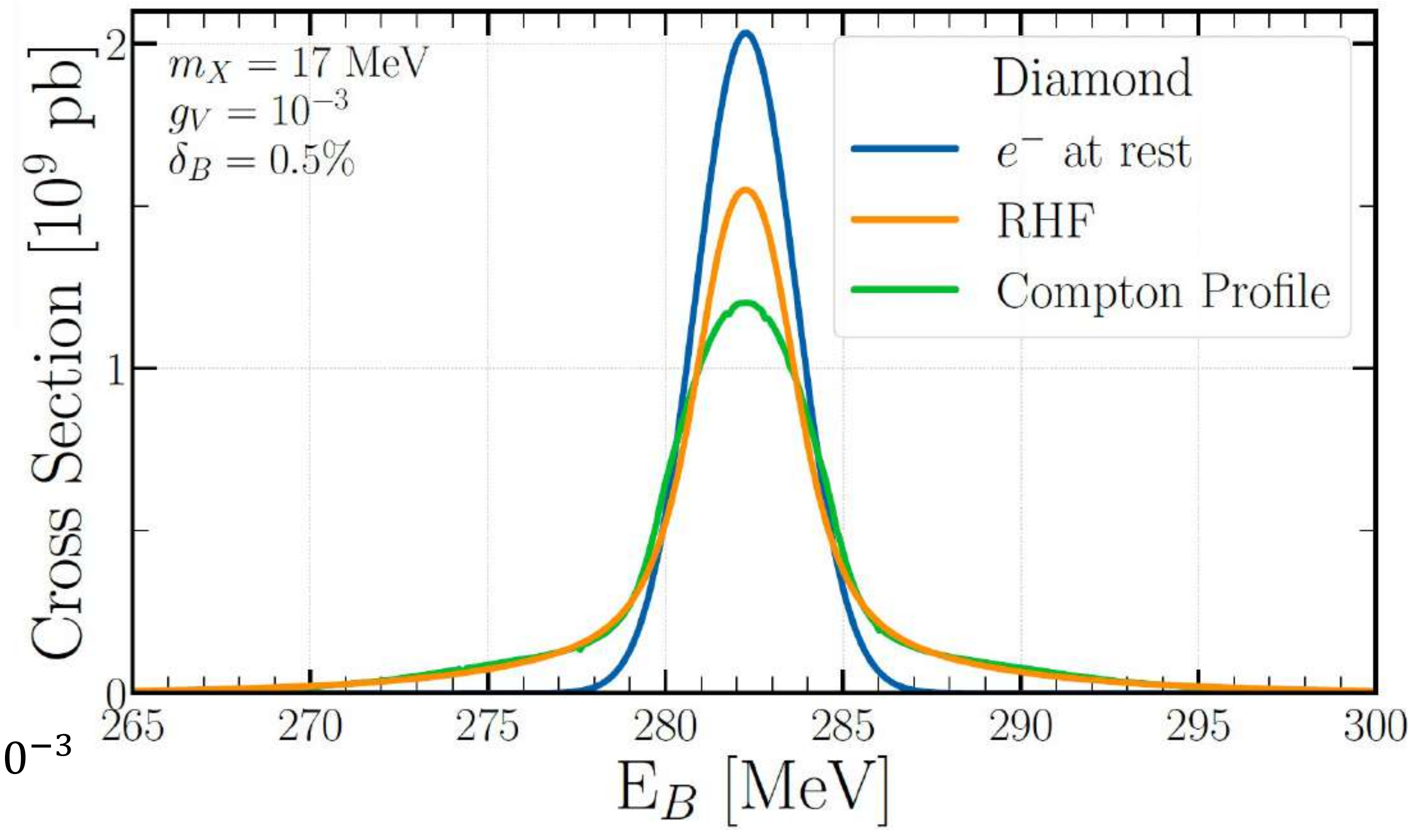

Sources of systematics

- Relative N^{PoT} estimation $\mathcal{O}(0.5\%)$
- Acceptance uncertainty $\sim 0.75\%$
- Beam energy spread $< 0.5\%$
- Signal shape uncertainty
- Beam condition
- Time dependent ECal efficiency
- Beam energy uncertainty - controlled by Hall probes < 10^{-3}
- ECal calibration

Normalization systematics

- absolute $N^{PoT} \sim 5\%$

PADME MC sensitivity estimate for Run III

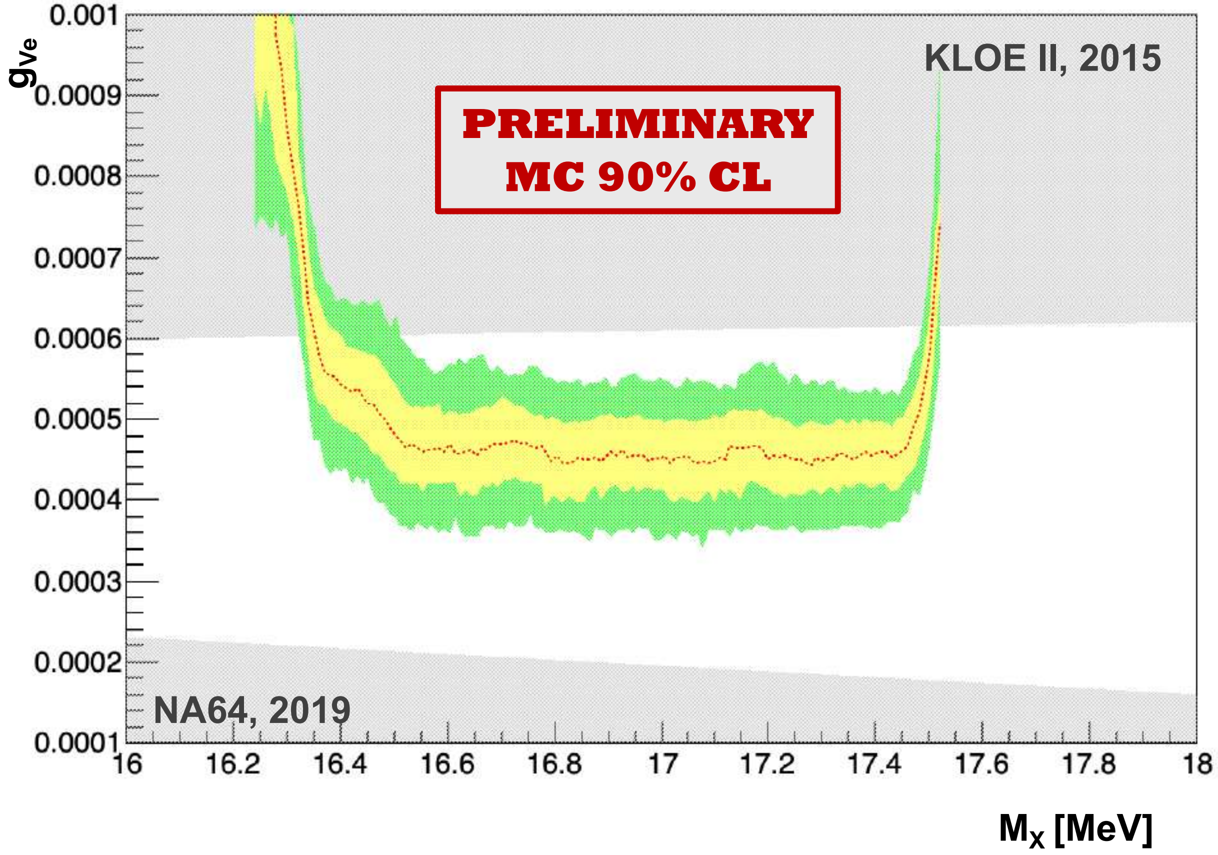

MC Expected 90% CL exclusion obtained using 0.9% systematic uncertainty

Expected 90% CL upper limits are obtained with the CLs method:

- Modified frequentist approach, LEP-style test statistic
- Likelihood fits performed for the separate assumptions of **signal + background vs background only**
- $Q_{statistics} = -2\ln\left(\frac{L_{sb}}{L_b}\right)$
- Pseudo data (SM background) is generated accounting for the expected uncertainties of nuisance parameters + statistical fluctuations
- **146 Nuisance parameters**:
  - N^{PoT} of each scan point
  - Common error on N^{PoT} (scale error)
  - Signal efficiency for each scan point
  - Background yield for each scan point
  - Signal shape parameters: theoretical input and beam energy spread

Conclusions

- PADME performed 53 (47 on-resonance + 6 off-resonance) cross section measurements of the SM allowed processes: Bhabha scattering and $\gamma\gamma$-production
- Quality of the Run III data meet expectations for X_{17} searches
  - $< 1\%$ systematic error is achievable
- Data are still blind, but PADME aims to set limits on both **vector** and **pseudoscalar** model
- The presence of the electron motion effect worsened the global significance for the X_{17} search, but the new effect could be exploit to improve BSM searches
- A new Run period (PADME Run IV) is already scheduled at the beginning of 2025
  - Collect x2 Run III data sample to close the gap in vector model parameter space
  - In case an excess is observed on Run III data sample → Focused Run IV in restricted $\sqrt{s}$ range

Conclusions

- PADME performed 53 (47 on-resonance + 6 off-resonance) cross section measurements of the SM allowed processes: Bhabha scattering and $\gamma\gamma$-production
- Quality of the Run III data meet expectations for X_{17} searches
  - $< 1\%$ systematic error is achievable
- Data are still blind, but PADME aims to set limits on both **vector** and **pseudoscalar** model
- The presence of the electron motion effect worsened the global significance for the X_{17} search, but the new effect could be exploit to improve BSM searches
- A new Run period (PADME Run IV) is already scheduled at the beginning of 2025
  - Collect x2 Run III data sample to close the gap in vector model parameter space
  - In case an excess is observed on Run III data sample → Focused Run IV in restricted $\sqrt{s}$ range

Thank you for your attention
Stay tuned!

BACKUP SLIDES

The X_{17} particle

According to the ATOMKI observations, the main properties of the new X_{17} particle are:

- $m_{X_{17}} \sim 17$ MeV
- $Br(e^+e^- \to X_{17}) \simeq 5{\times}10^{-6} Br(e^+e^- \to \gamma\gamma)$
- $\Gamma_V = 0.5 \left(\frac{g_V}{0.001}\right)^2$ eV for the vector case

The spin-parity selection rules $J_* = L \oplus J_0 \oplus J_X$ and $P_* = (-1)^L \, P_0 P_X$ are required to identify the nature of the new mediator

As proposed by *J. Feng in Phys.Rev.D* 102 (2020) 3, 036016

N_*	J_*^P	Scalar X17	Pseudoscalar X17	Vector X17	Axial Vector X17
^{8}Be(18.15)	1^+	✗	✓	✓	✓
^{12}C(17.23)	1^-	✓	✗	✓	✓
^{4}He(21.01)	0^-	✗	✓	✗	✓
^{4}He(20.21)	0^+	✓	✗	✓	✗

^{12}C Last results

Phys. Rev. C 106, L061601

The accessible observables @PADME Run III

Goal: keep at the % level the systematic error

$\frac{N(e^+e^-)}{N^{PoT}}$ vs $\sqrt{s}$ & $\frac{N(\gamma\gamma)}{N^{PoT}}$ vs $\sqrt{s}$ → vector/pseudoscalar nature of X_{17}

- Systematic errors due to ETag tagging efficiency stability and N^{PoT}

$\frac{N(e^+e^-+\gamma\gamma)}{N^{PoT}}$ vs $\sqrt{s}$ → existence of X_{17}

- High statistical significance (small sensitivity loss due to small only 20% $\gamma\gamma$-production bkg)
- No ETag related systematic errors

$\frac{N(e^+e^-)}{N(\gamma\gamma)}$ vs $\sqrt{s}$ → existence of X_{17}

- Lower statistical significance due to smaller $\gamma\gamma$ cross section
- Do not depend N^{PoT} → error dominated by tagging efficiency

Components in the analysis:

- Signal selection and events identification → Bkg contribution
- Determination of the normalization → PADME beam measurement
- Expected signal yield → Theoretical input: X_{17} line shape

Current limits on X_{17} from leptons

Phys. Rev. D 101, 071101 (R) (2020)

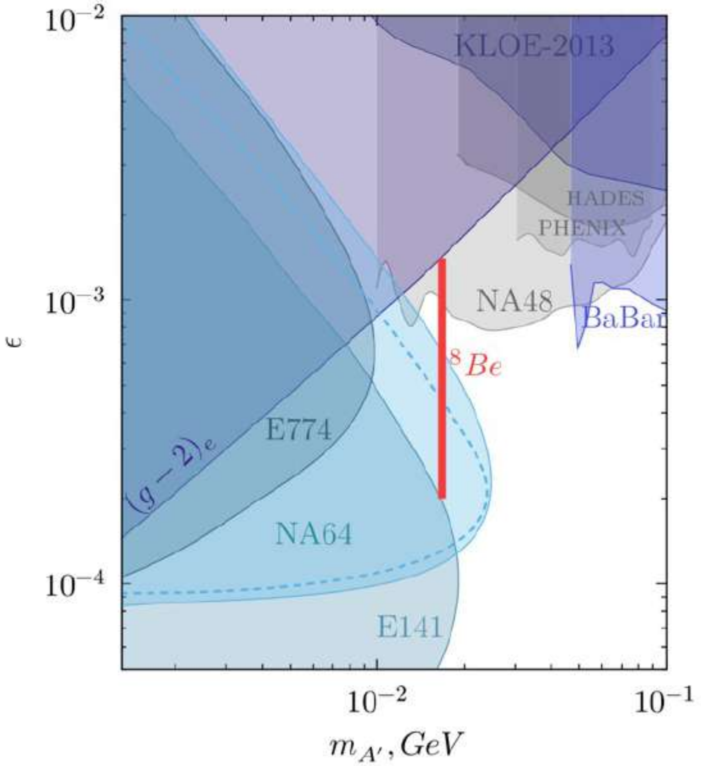

Phys. Rev. D 104, L111102 (2021)

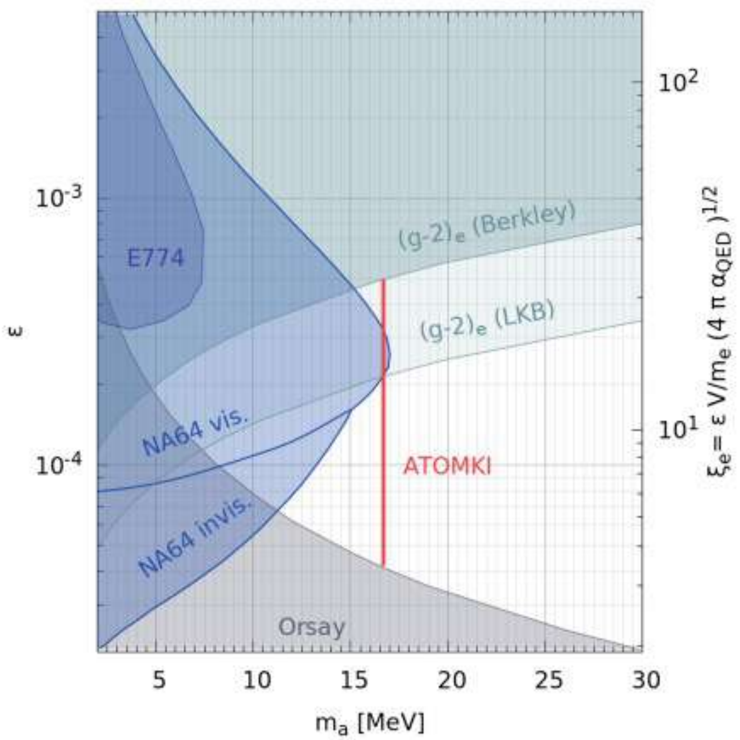

X_{17} as a vector particle:

- LKB $(g\text{-}2)_e$ bound weaker for vector and model dependent
- NA48/2 bound not valid for "protophobic" X_{17}
- Still a lot of free parameter space for vector X_{17}

X_{17} as pseudoscalar particle:

- $(g\text{-}2)_e$ bound stronger for pseudo scalars
- Still model dependent and with big data uncertainties
- Almost unconstrained parameter space for X_{17}

PADME Run I & II setup

PADME is based @Laboratori Nazionali di Frascati (LNF) and it searches for A' in the associated production $e^+e^- \to \gamma A'$

- e^+-beam ($E < 550$ MeV) on 100μm active diamond target
- Dipole B-field bends out the un-interacted beam and charged particles
- Signal→ 1γ in BGO Electromagnetic Calorimeter (ECal) & nothing elsewhere, measuring ΔM^2_{miss} and giving us access to $m_{A'}$
- Bremsstrahlung rejected by ECal hole and the Small Angle Calorimeter (SAC) immediately behind
- Plastic scintillator bars as charged particle vetoes

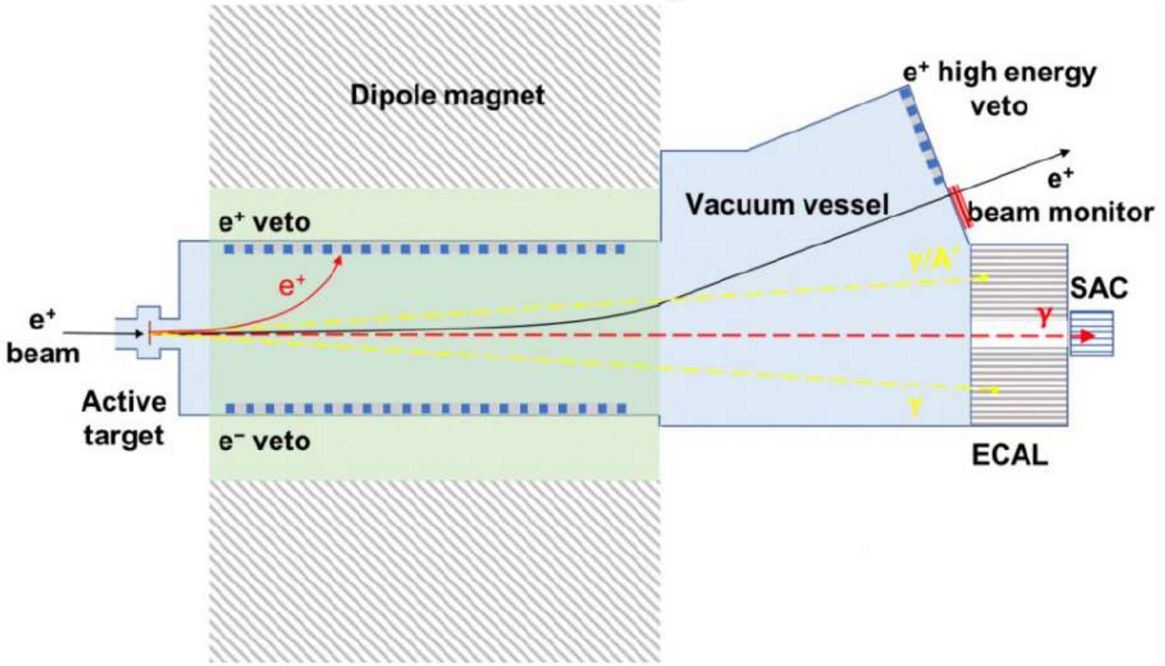

P. Albicocco et al 2022 JINST 17 P08032

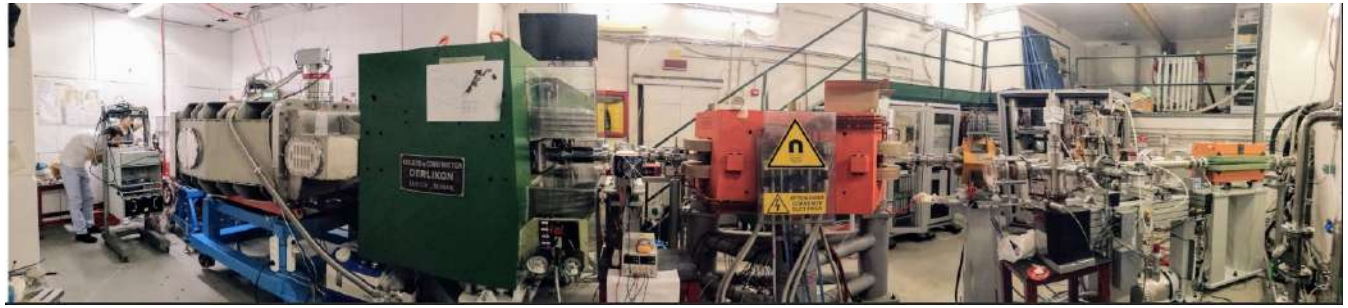

Run I and II data taking

Two Runs in three configurations between September 2018 and December 2020

Acquired luminosities:

- Run I → $7{\times}10^{12}\ PoT$
- Run II → $5.5{\times}10^{12}\ PoT$
- Multiplicity $N_{bunch}^{PoT} \simeq 3{\times}10^{4}$

Changes between the first two runs:

- Run Ia: secondary beam → Run Ib: primary beam
  → Reduced BIB
- Run Ib → Run II: changed the vacuum separation
  → Reduced BG from vacuum window
- Run Ib → Run II: longer beam (250 → 280 ns)
  → Reduced the pile-up in detectors

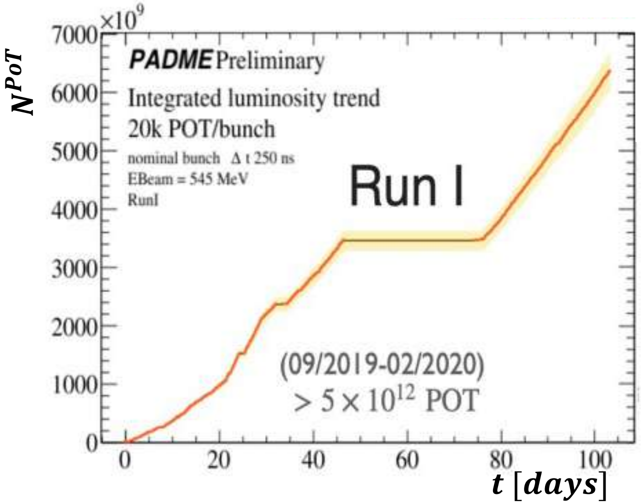

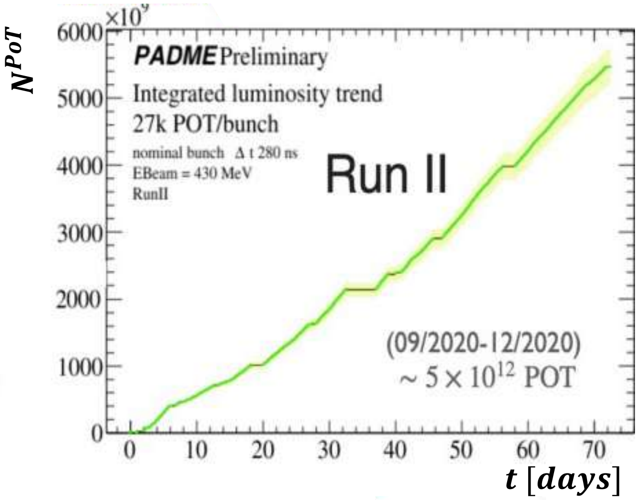

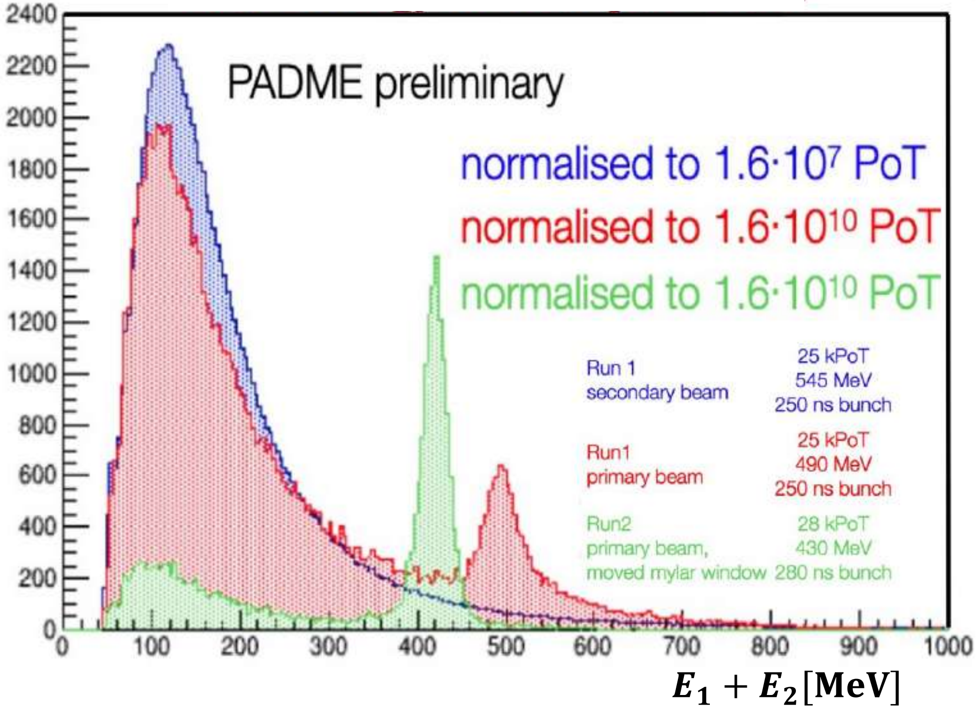

The Multiphoton annihilation measurement

From the $\sigma(e^+e^- \to \gamma\gamma\ (\gamma))$ measurement:

- Characterisation of ECal
- $\sigma(e^+e^- \to \gamma A') \propto g_V^2 \times \sigma(e^+e^- \to \gamma\gamma) \times \delta(M_{A'})$
- Could be sentisitive to sub-GeV new physics (e.g. ALPs)

First measurement below $500\ \mathrm{MeV}$ with $< 20\%$ precision with only 10% of Run II dataset

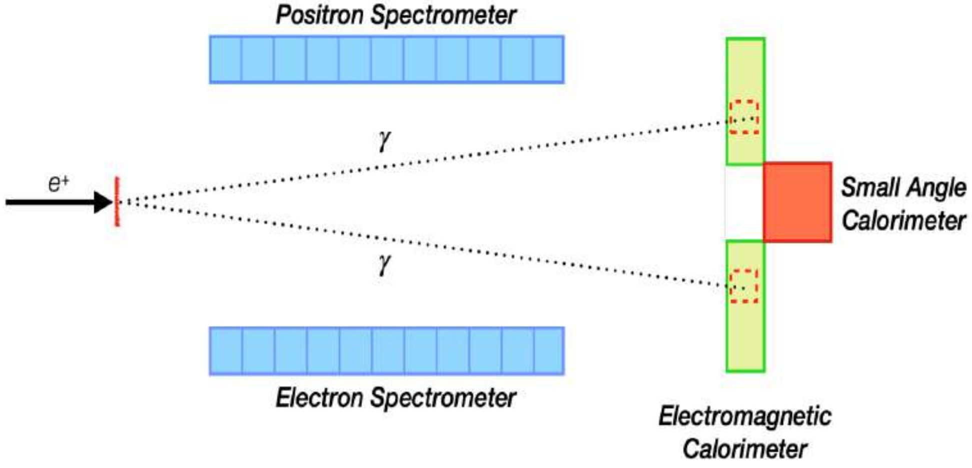

F. Bossi *et al.* Phys. Rev. D **107**, 012008

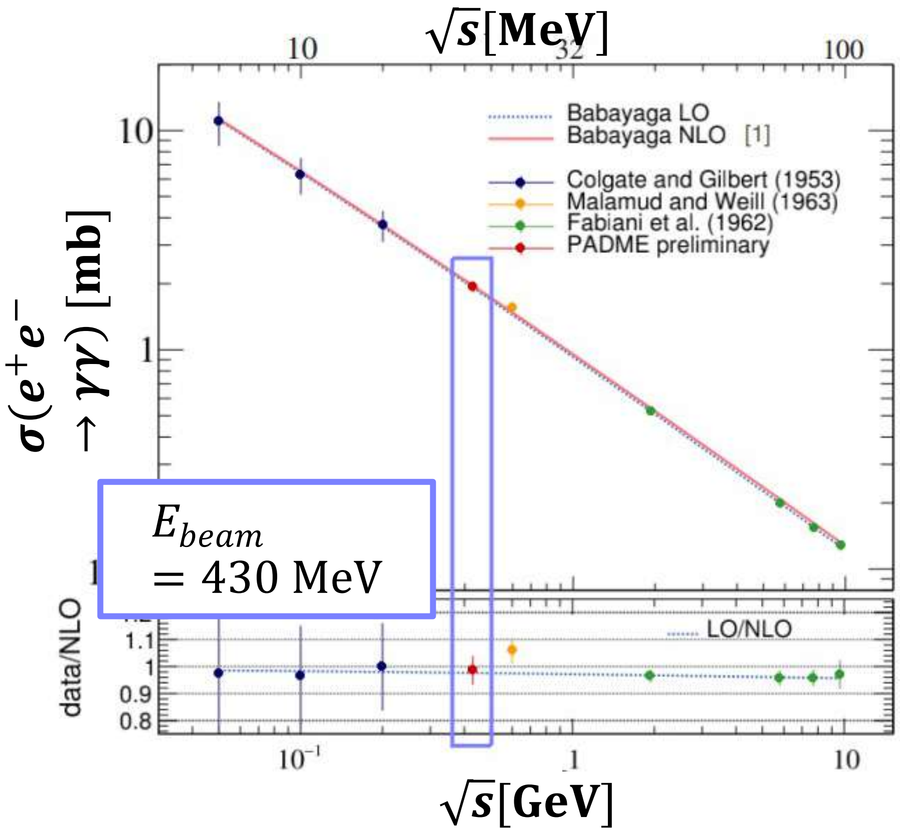

PADME → $\boldsymbol{\sigma(e^+e^- \to \gamma\gamma\ (\gamma)) = 1.930 \pm 0.029_{stat} \pm 0.057_{syst} \pm 0.020_{target} \pm 0.079_{lumi}\ \mathrm{mb}}$

QED@NLO $\sigma(e^+e^- \to \gamma\gamma\ (\gamma)) = 1.9573 \pm 0.0005_{stat} \pm 0.0020_{syst}\ \mathrm{mb}$ *Phys.Lett.B* 663 (2008) 209-213

Strategy N_{ee}/N_{gg}

The results from PADME RUN III will be dominated by PoT systematics, two clusters acceptance acceptance systematics

- Exploit a different normalization channel which could possibly cancel part of the systematic effects

Natural candidate: $e^+e^- \rightarrow \gamma\gamma$

- Same 2 body kinematics: similar ECal illumination, systematics due to bad ECal crystals largely cancels

Back on the envelope estimation: need knowledge of $N_{\gamma\gamma}$ at 0.5 % for each scanning point

- $\sigma(e^+e^- \rightarrow \gamma\gamma)_{E=300\ \mathrm{MeV}} \sim 2$ mb, Acc $(e^+e^- \rightarrow \gamma\gamma) \sim 10$ % $\Rightarrow$ O(10k) $\gamma\gamma$ events per 10^{10} PoT
    - Need 4 times higher statistics per scan point
- Less scan points due to the widening of X17 lineshape because of the electronic motion
- Higher intensity – by a factor of 2

Need good separation between charged and neutral final states

Courtesy of V. Kozhuharov

Courtesy of V. Kozhuharov

Positron flux measurement

arXiv:2405.07203 [hep-ex]

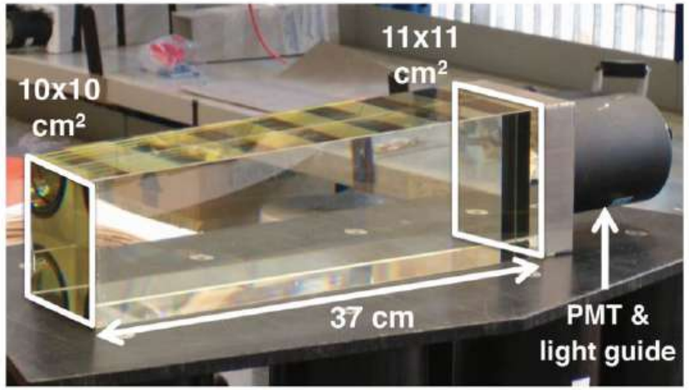

- PoT is primarily measured by an OPAL lead glass block downstream of the setup
- Additional detectors to control the PoT systematics
  - and to derive correction factors
- Several testing campaigns
  - A few positrons -> clear 1e, 2e, etc. peak identification
  - O(2000) PoT - cross-calibration with the FitPix

- Higher energy runs
  - control of the NPoT systematics
  - 2 clusters selection stability

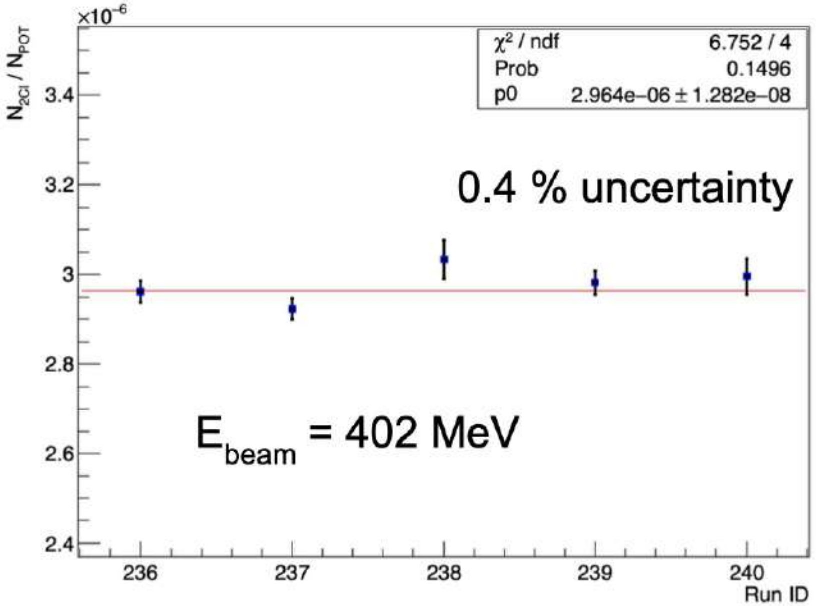

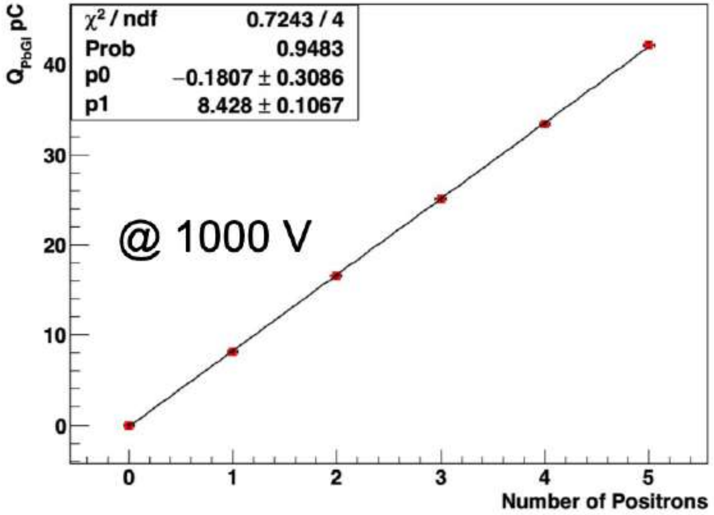

$Q_{1e} = (8.24 \pm 0.021_{Stat} \pm 0.12_{Syst})$ pC

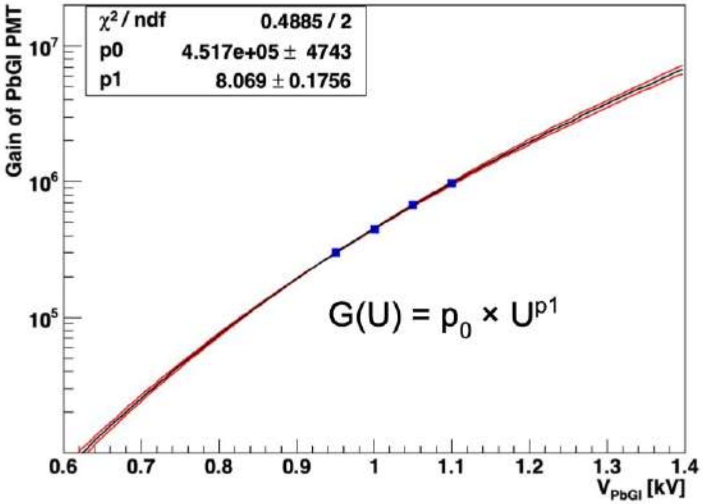

G (650V) = (14001 ± 1121)

8 % uncertainty on NPoT

NOTE: consider more points for gain curve determination

arXiv:2405.07203

Courtesy of V. Kozhuharov

Absolute positron flux measurement

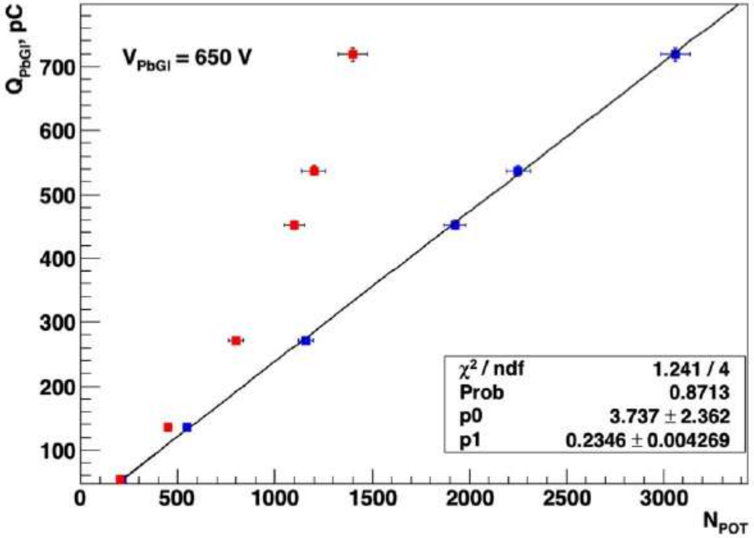

- Calibration of the lead glass @ 650 V with respect to the BTF FitPix
- Correction applied to the FitPix data to account for the high positron density

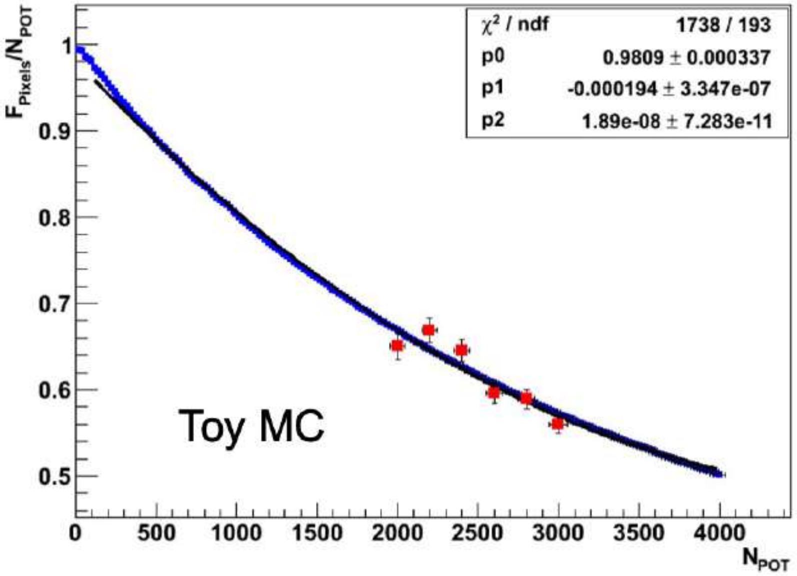

- Validation of the toy MC (and F_{pixel} correction factor) with an independent measurement from BTF luminometer
- Correction uncertainty - of the order of 1 %
  - Common to all the measurements

$$Q_{1e} = (0.235 \pm 0.0043)\ \mathrm{pC}$$

- Uncertainty on Q_{1e}: < 2%

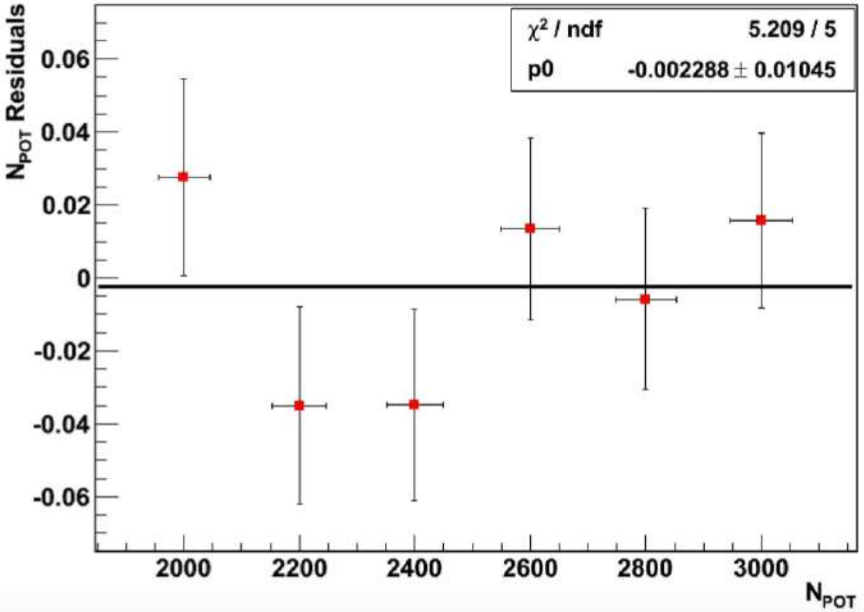

arXiv:2405.07203

Courtesy of V. Kozhuharov

Positron flux measurement

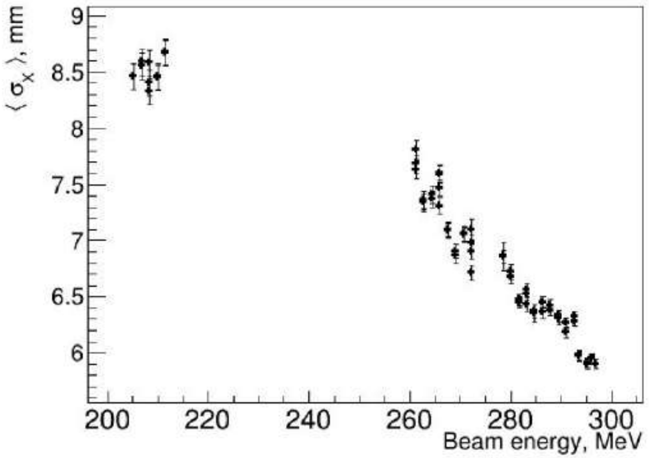

- The beam spread in Y direction varies within ~2 mm during the data taking
- The beam spread in X is energy dependent
  - However in X the containment is largely ensured

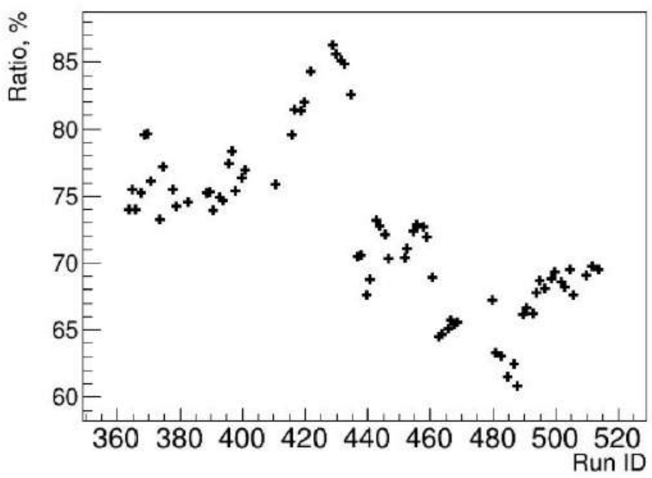

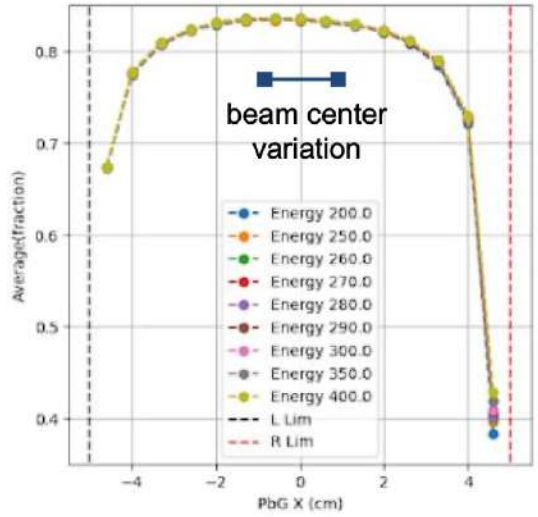

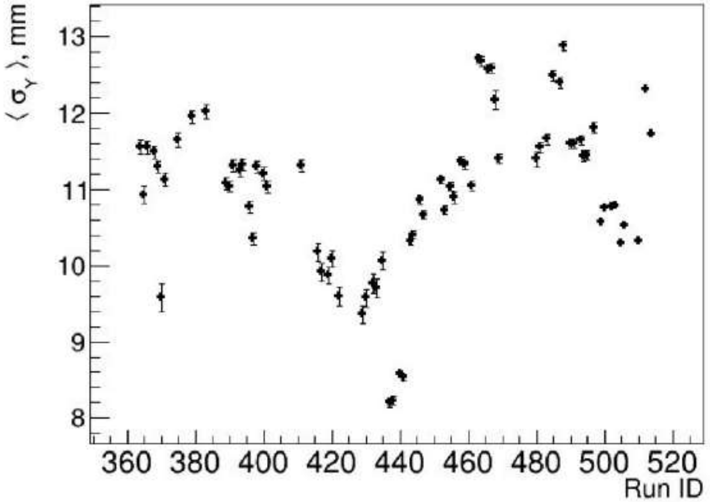

Correction due to the beam movement (convolution of TimePix & LeadGlass) results in systematics contribution < 1 %

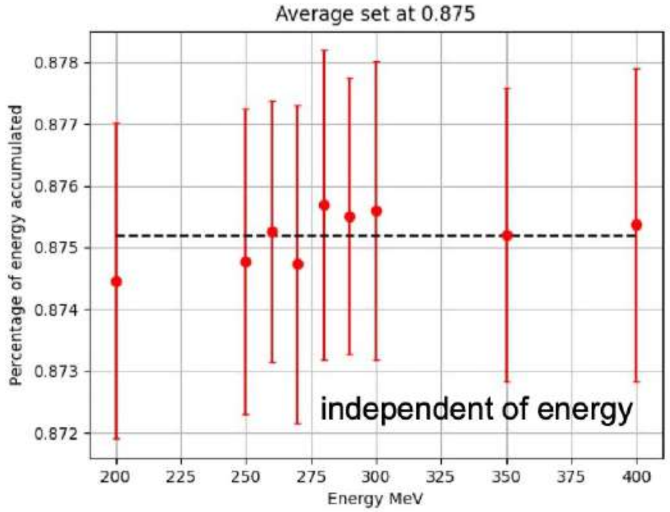

The energy containment correction uncertainty well below 1 %

arXiv:2405.07203

Courtesy of V. Kozhuharov

Strategy: $N_{e+e-}/N_{\gamma\gamma}$

- e^+e^- tagging with high efficiency
  - And well controlled mis-tagging probability
- Micromegas tagger – double sided readout gas chamber with X/Y readout

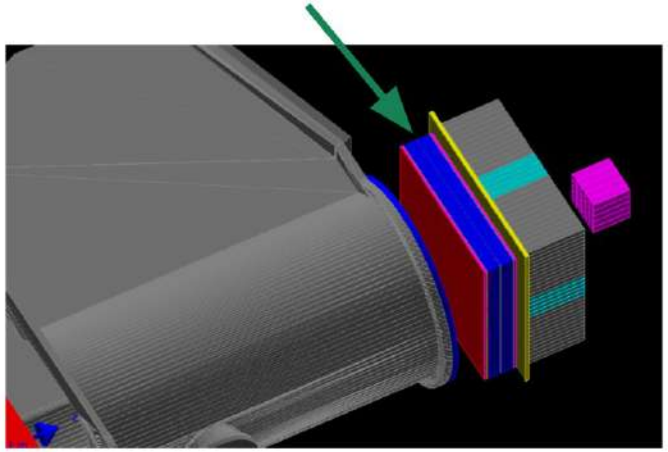

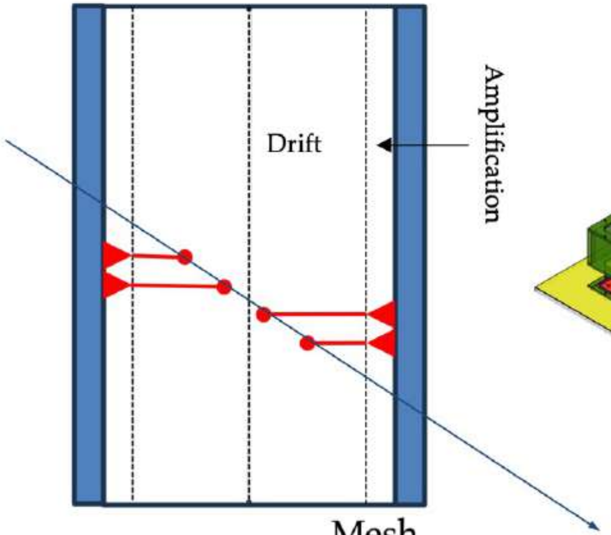

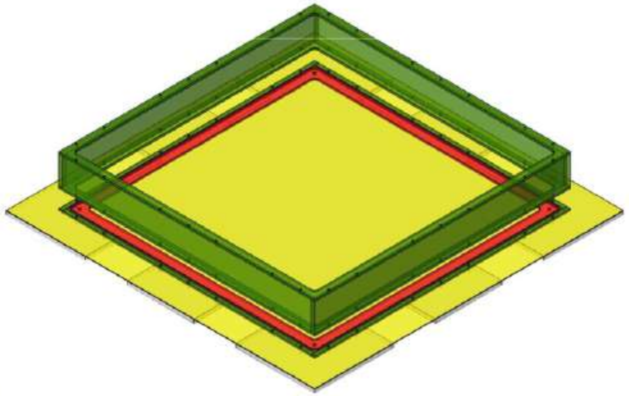

Testbeam results, tracking at 22 degrees

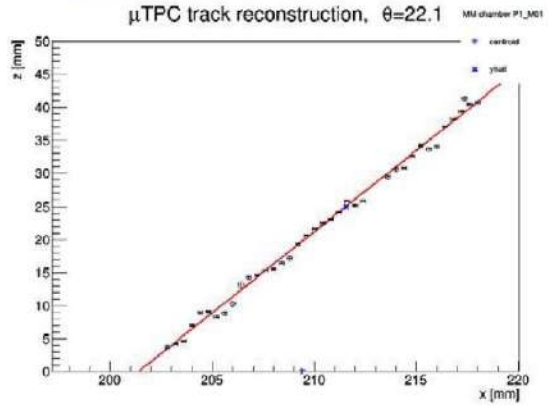

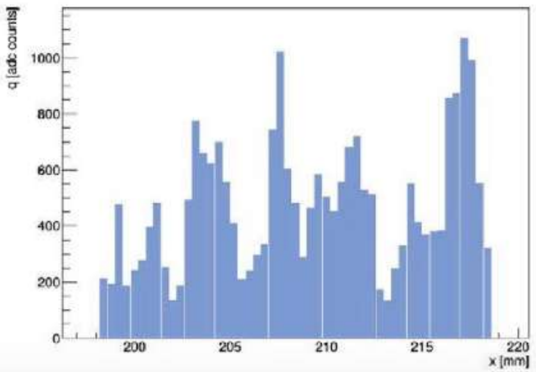

- Installing a new detector in the PADME setup due to rate limitations of the present tagger
- A completely new detector technology to be used in PADME
  - Gaining expertise and manpower from LNF ATLAS group

Courtesy of V. Kozhuharov

PADME tagger

- A novel micromegas readout plane suggested
  - Rhomboidal pads for X and Y direction, decrease the mutual capacitance
- Variable HV depending on the distance from the beam center
  - Low HV in the center, measure the beam multiplicity
    - Additional control on the PoT
  - Higher HV in periphery to ensure close to 100 % efficiency

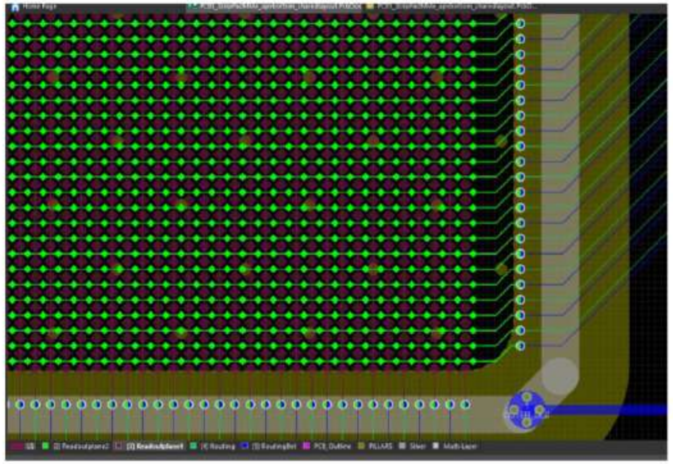

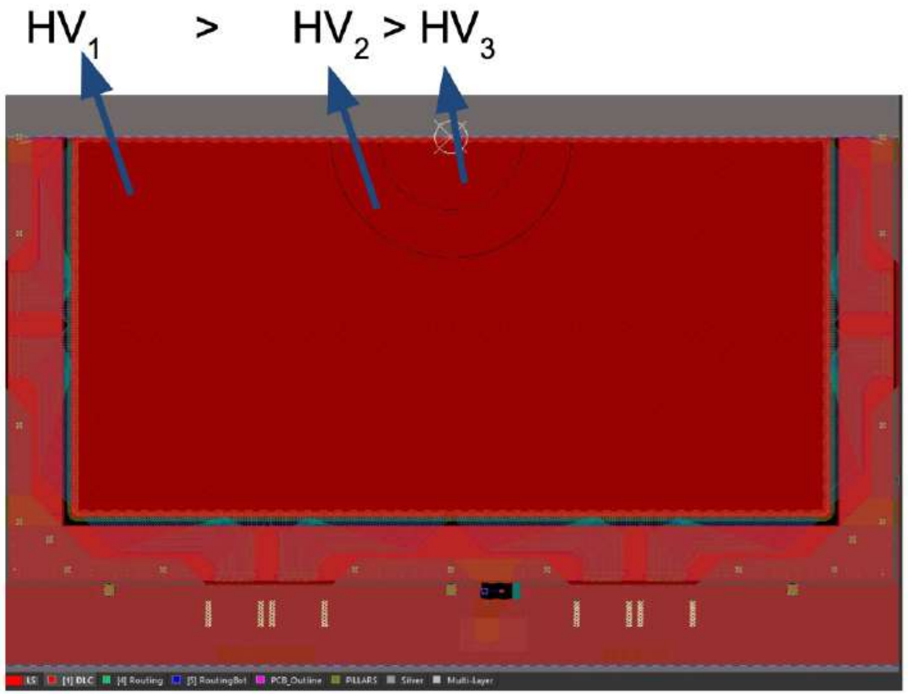

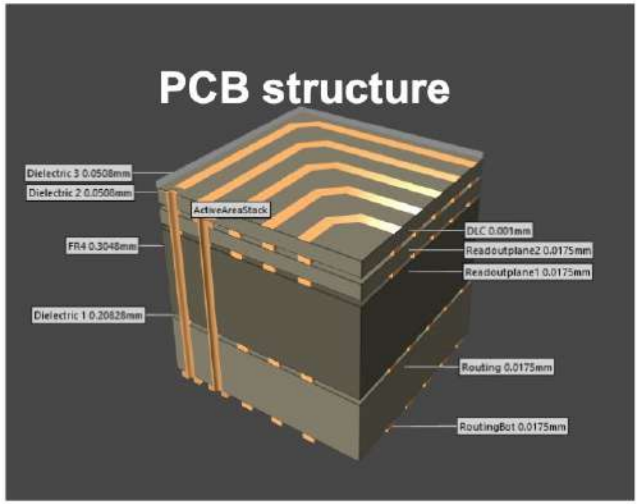

- Gas mixture:
  $Ar{:}CF_4{:}i\text{-}C_4H_{10} = 88{:}10{:}2$
- Readout - SRS system with APV ASIC hybrid
  - An adapter card in preparation to allow APV25 to accept/record trigger signal
  - Timing and event matching

Status

- PCBs under preparation, to be ready for assembly in July
- Readout exists, integration with PADME DAQ ongoing (online vs offline)
- Gas supplies - premixed gas (7-10 days) vs gas mixer in BTFEH1